



## PM<sub>2.5</sub> pollution in a megacity of southwest China: source apportionment and implication

J. Tao<sup>1</sup>, J. Gao<sup>2</sup>, L. Zhang<sup>3</sup>, R. Zhang<sup>4</sup>, H. Che<sup>5</sup>, Z. Zhang<sup>1</sup>, Z. Lin<sup>1</sup>, J. Jing<sup>6</sup>, J. Cao<sup>7</sup>, and S.-C. Hsu<sup>8</sup>

<sup>1</sup>South China Institute of Environmental Sciences, Ministry of Environmental Protection, Guangzhou, China

<sup>2</sup>Chinese Research Academy of Environmental Sciences, Beijing, China

<sup>3</sup>Air Quality Research Division, Science Technology Branch, Environment Canada, Toronto, Canada

<sup>4</sup>RCE-TEA, Institute of Atmospheric Physics, Chinese Academy of Sciences, Beijing, China

<sup>5</sup>Key Laboratory of Atmospheric Chemistry (LAC), Institute of Atmospheric Composition, Chinese Academy of Meteorological Sciences (CAMS), China

<sup>6</sup>Centre for Atmosphere Watch and Services (CAWAS), Meteorological Observation Center of CMA, Beijing, China

<sup>7</sup>Key Laboratory of Aerosol, SKLLQG, Institute of Earth Environment, Chinese Academy of Sciences, Xi'an, China

<sup>8</sup>Research Center for Environmental Changes (RCEC), Academia Sinica, Taipei, Taiwan

Correspondence to: S.-C. Hsu (schsu815@rcec.sinica.edu.tw) and J. Gao (gaojian@craes.org.cn)

Received: 7 January 2014 – Published in Atmos. Chem. Phys. Discuss.: 25 February 2014

Revised: 20 June 2014 – Accepted: 9 July 2014 – Published: 26 August 2014

**Abstract.** Daily PM<sub>2.5</sub> (aerosol particles with an aerodynamic diameter of less than 2.5 μm) samples were collected at an urban site in Chengdu, an inland megacity in southwest China, during four 1-month periods in 2011, with each period in a different season. Samples were subject to chemical analysis for various chemical components ranging from major water-soluble ions, organic carbon (OC), element carbon (EC), trace elements to biomass burning tracers, anhydro-sugar levoglucosan (LG), and mannosan (MN). Two models, the ISORROPIA II thermodynamic equilibrium model and the positive matrix factorization (PMF) model, were applied to explore the likely chemical forms of ionic constituents and to apportion sources for PM<sub>2.5</sub>. Distinctive seasonal patterns of PM<sub>2.5</sub> and associated main chemical components were identified and could be explained by varying emission sources and meteorological conditions. PM<sub>2.5</sub> showed a typical seasonality of waxing in winter and waning in summer, with an annual mean of 119 μg m<sup>-3</sup>. Mineral soil concentrations increased in spring, whereas biomass burning species elevated in autumn and winter.

Six major source factors were identified to have contributed to PM<sub>2.5</sub> using the PMF model. These were secondary inorganic aerosols, coal combustion, biomass burning, iron and steel manufacturing, Mo-related industries, and soil dust, and they contributed 37 ± 18, 20 ± 12, 11 ± 10,

11 ± 9, 11 ± 9, and 10 ± 12 %, respectively, to PM<sub>2.5</sub> masses on annual average, while exhibiting large seasonal variability. On annual average, the unknown emission sources that were not identified by the PMF model contributed 1 ± 11 % to the measured PM<sub>2.5</sub> mass. Various chemical tracers were used for validating PMF performance. Antimony (Sb) was suggested to be a suitable tracer of coal combustion in Chengdu. Results of LG and MN helped constrain the biomass burning sources, with wood burning dominating in winter and agricultural waste burning dominating in autumn. Excessive Fe (Ex-Fe), defined as the excessive portion in measured Fe that cannot be sustained by mineral dust, is corroborated to be a straightforward useful tracer of iron and steel manufacturing pollution. In Chengdu, Mo / Ni mass ratios were persistently higher than unity, and considerably distinct from those usually observed in ambient airs. V / Ni ratios averaged only 0.7. Results revealed that heavy oil fuel combustion should not be a vital anthropogenic source, and additional anthropogenic sources for Mo are yet to be identified. Overall, the emission sources identified in Chengdu could be dominated by local sources located in the vicinity of Sichuan, a result different from those found in Beijing and Shanghai, wherein cross-boundary transport is significant in contributing pronounced PM<sub>2.5</sub>. These results provided implications for PM<sub>2.5</sub> control strategies.

## 1 Introduction

Fine particulate matter (PM<sub>2.5</sub>) – those particles with an aerodynamic diameter of less than 2.5 μm – is a key air pollutant in terms of adverse human health effects and visibility degradation (Pope III and Dockery, 2006; Watson, 2002). The specialized cancer agency of the World Health Organization (WHO), the International Agency for Research on Cancer (IARC), has classified outdoor PM as carcinogenic to humans (Group 1) (<http://www.iarc.fr/>). For instance, daily mortality has been found to be related to the level of PM<sub>2.5</sub> sourced from traffic emission and coal combustion in six US cities (Laden et al., 2000). PM<sub>2.5</sub> is a complex mixture of sulfate (SO<sub>4</sub><sup>2-</sup>), nitrate (NO<sub>3</sub><sup>-</sup>), ammonium (NH<sub>4</sub><sup>+</sup>), water (H<sub>2</sub>O), organic and element carbon (OC and EC), soil dust, trace elements, and persistent organic pollutants (Seinfeld et al., 2004; Zhang et al., 2013). It originates from both natural and anthropogenic sources, and includes both primary and secondary particle species. Knowledge of sources and their contributions to PM<sub>2.5</sub> is crucial in making feasible policies for controlling PM<sub>2.5</sub> levels to protect human health and reduce the occurrence of hazy weather.

Source apportionment of PM<sub>2.5</sub> has been achieved extensively around the world (Lee and Kang, 2001; Putaud et al., 2004; Hueglin et al., 2005; Lonati et al., 2005; Chen et al., 2010). Such a technique has been increasingly applied for the past decade in China, although mostly focused on urban cities and areas such as Beijing, the Yangtze River delta (YRD), and the Pearl River delta (PRD) (He et al., 2001; Ye et al., 2003; Tao et al., 2012; Zhang et al., 2013). To date, PM<sub>2.5</sub> pollution is still a severe problem in China. The Sichuan Basin is one of the most polluted regions in China (Cao et al., 2007; Zhao et al., 2010; Yang et al., 2011), as demonstrated by the spatial distribution of aerosol optical depth (AOD) retrieved by satellites (Fig. 1; Remer et al., 2005).

Chengdu, located west of the Sichuan Basin (Fig. 1), is one of the megacities in China with a population of more than 10 million. This megacity is one of the few inland megacities worldwide which are far from oceans. Air pollution is a serious issue for this city, presumably due to the complex topography surrounding the city and huge amounts of coal consumption (Tao et al., 2013). For example, PM<sub>2.5</sub> concentrations reached an annual mean of 165 μg m<sup>-3</sup> in 2009 to 2010, which is 5 times higher compared with the new national ambient air quality standards (NAAQS) (35 μg m<sup>-3</sup>) and 16 times higher compared with the air quality guideline (10 μg m<sup>-3</sup>) recommended by the WHO (Tao et al., 2013). Achieving NAAQS in this city is apparently a challenging task. A better understanding of PM<sub>2.5</sub> sources and their relative contributions is urgently needed to enact effective emission control policies and to implement multi-pollutant reduction measures. To date, studies on seasonal-based source apportionments remain lacking, yet they are critical in shedding light on emission control measures of air pollutants and

in creating emission control policies (Tao et al., 2013). To fill these gaps, a comprehensive data set acquired in 2011 is analyzed in the present study, with an emphasis on seasonal-based source apportionments.

Accordingly, the present study aims to accomplish the following goals: to systematically characterize PM<sub>2.5</sub> levels and their chemical compositions on seasonal and annual basis, to identify PM<sub>2.5</sub> source factors and to quantify their respective contributions, and to evaluate existing and recommend new environmental protection measures based on novel source apportionment results.

## 2 Methodology

### 2.1 Site description

PM<sub>2.5</sub> samples were collected at the Chengdu Research Academy of Environmental Sciences (CRAES) located in the urban area of Chengdu (30.65° N, 104.03° E) (Fig. 1). Instruments used in this study were installed on the roof (21 m above ground) of an office building of CRAES. This site was built with unimpeded vision, although a residential area and a park were situated about 100 m east of the sampling site. In 2004, the Chengdu municipal government promulgated the “Chengdu Plan of Industrial Development Layout (2003–2020)”, which forbids any pollution industries within the third-ring road inside the city (<http://www.cdgy.gov.cn/Article/2004/200402/1165.html>). The CRAES site is within and more than 5 km away from the third-ring road (Supplement Fig. S1). Therefore, no major stationary air pollution sources were present within a circumference of 5 km of the site, except mobile emissions; however, the site was affected by industrial pollution outside the third-ring road. Thus, the site was considered to be representative of a typical urban environment in Chengdu.

### 2.2 Sampling

PM<sub>2.5</sub> samples were collected using two low-flow air samplers (MiniVol TAC, AirMetrics Corp., Eugene, OR, USA). Prior to the start of the sampling campaign, the flow rate of PM<sub>2.5</sub> samplers was calibrated. Samples were collected at a flow rate of 5 L min<sup>-1</sup> on two types of filters: a 47 mm quartz fiber filter (Whatman QM-A) and a 47 mm Teflon filter (Whatman PTFE). Quartz filters were pre-baked at 800 °C for 3 h prior to sampling. Collected filters were stored in a freezer at -18 °C before chemical analysis to minimize evaporation of volatile components.

A total of 117 PM<sub>2.5</sub> samples along with 12 blank samples were collected in 2011 during the following periods: 6–30 January (representative of winter), 3 April–3 May (spring), 1–31 July (summer), and 1–31 October (autumn). Collection duration of each sample was 24 h, starting at 10:00 local time (LT) each day and ending at 10:00 LT the following day. Three field blanks were collected with each sampler during

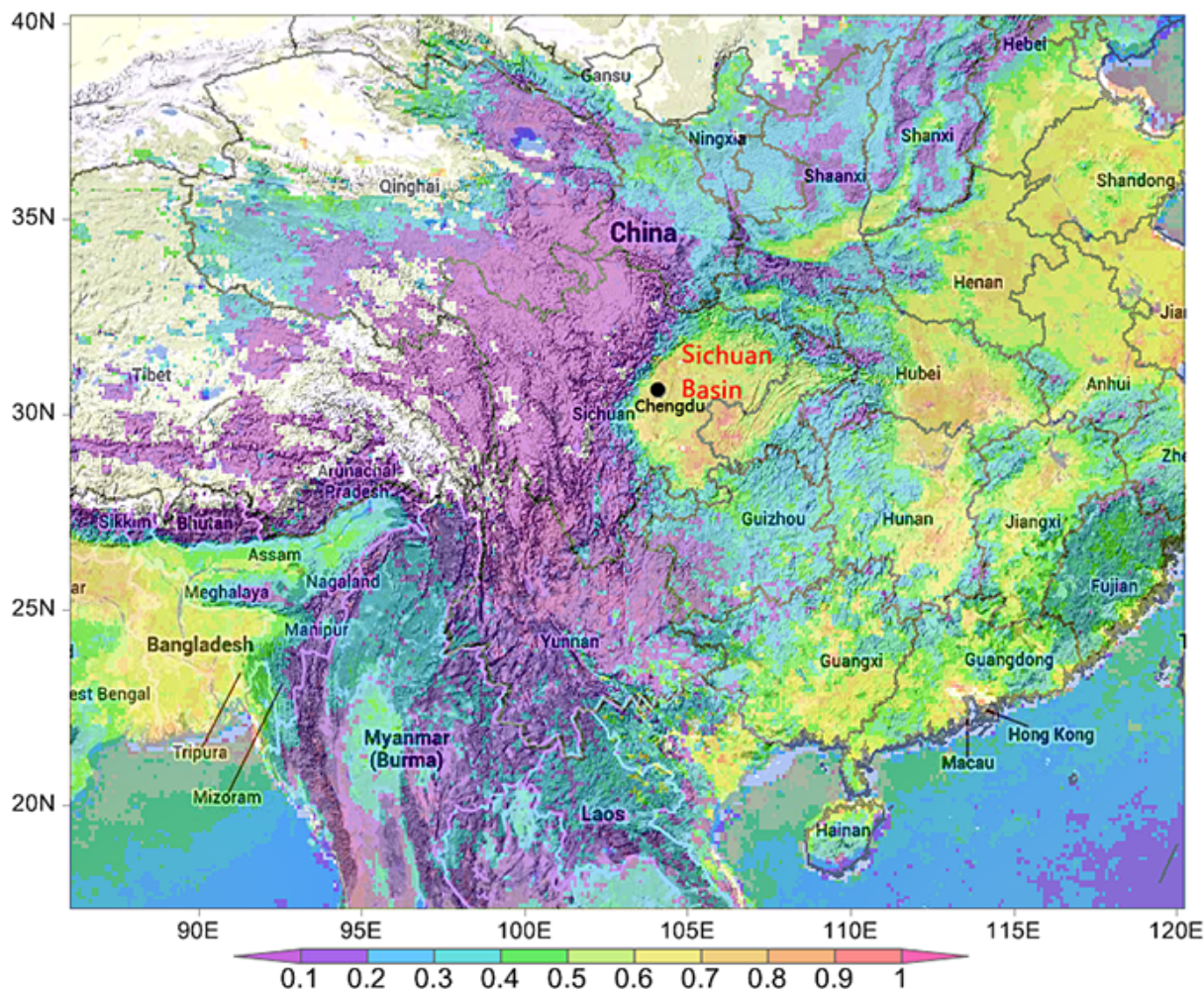


**Figure 1.** Sampling location ( $30.65^{\circ}$  N,  $104.03^{\circ}$  E) in Chengdu on a regional map superimposed with spatial distribution of annual mean aerosol optical depth (AOD) retrieved from Moderate Resolution Imaging Spectrometer (MODIS) satellite remote sensing in 2011.

every seasonal campaign, which were then analyzed together with the samples.

### 2.3 Gravimetric weighing

Teflon filters were measured gravimetrically for particle mass concentration using a Sartorius MC5 electronic microbalance with a sensitivity of  $\pm 1 \mu\text{g}$  (Sartorius, Göttingen, Germany) after 24 h equilibration at  $23 \pm 1^{\circ}\text{C}$  with relative humidity at  $40 \pm 5\%$ . Each filter was weighed at least three times before and after sampling. Differences among replicate weights were mostly less than  $20 \mu\text{g}$  for each sample. Net mass was obtained by subtracting pre-weight from post-weight.

## 2.4 Chemical analysis

### 2.4.1 OC and EC

An area of  $0.526 \text{ cm}^2$  punched from each quartz filter was analyzed for eight carbon fractions following the IMPROVE\_A thermal/optical reflectance (TOR) protocol on a DRI model 2001 carbon analyzer (Atmoslytic Inc., Calabasas, CA, USA) (Chow et al., 2007). This analysis acquired four OC fractions (OC1, OC2, OC3, and OC4 at 140, 280, 480, and  $580^{\circ}\text{C}$ , respectively, in a helium (He) atmosphere), OP (a pyrolyzed carbon fraction determined when transmitted laser light attains its original intensity after oxygen ( $\text{O}_2$ ) was added to the analysis atmosphere), and three EC fractions (EC1, EC2, and EC3 at 580, 740, and  $840^{\circ}\text{C}$ , respectively, in a 2%  $\text{O}_2$  / 98% He atmosphere). IMPROVE\_TOR OC is operationally defined as  $\text{OC1} + \text{OC2} + \text{OC3} + \text{OC4} + \text{OP}$  and EC is defined as  $\text{EC1} + \text{EC2} + \text{EC3} - \text{OP}$  (Chow et al., 2007).

Additional quality assurance (QA) and quality control (QC) procedures have been described in detail in Cao et al. (2003).

#### 2.4.2 Trace elements and water-soluble ions

Each PTFE filter was cut into two equal halves with ceramic scissors, and then subjected to extraction and digestion. One half was extracted with ultrapure water for ionic measurement and the other half was dissolved with acids for elemental measurement. Digestion was performed with an acid mixture (5 mL HNO<sub>3</sub> + 2 mL HF) by using an ultra-high throughput microwave digestion system (MARSPress, CEM, Matthews, NC). A blank reagent and two filter blanks were prepared in each run following the same procedures adopted for the samples. All acids used in this study were of ultrapure grade (Merck, Germany). The detailed digestion method can be found elsewhere (Hsu et al., 2008, 2010). A suite of trace elements in the digestion solutions – including Al, Fe, Na, Mg, K, Ca, Sr, Ba, Ti, Mn, Co, Ni, Cu, Zn, Mo, Ag, Cd, Sn, Sb, Tl, Pb, V, Cr, As, Y, Se, Zr, Nb, Ge, Rb, Cs, Ga, U, and 15 rare earth elements (REEs) – were analyzed by quadrupole-based inductively coupled plasma mass spectrometry (ICP-MS; Elan 6100, Perkin Elmer™ SCIEX, USA). Calibration was achieved using multielement standards prepared from stock standards (Merck) in 2% HNO<sub>3</sub> solution. Quality assurance and control (QA/QC) of ICP-MS measurement was guaranteed by the analysis of a certified reference standard, NIST SRM-1648 (urban particulates). Resulting recoveries fell within ±10% of the certified values for most elements, except for Se, As, Cs, Sb, and Rb (±15%) (Zhang et al., 2013). The precision for most elements is better than 5% ( $n = 5$ ).

Silicon was quantified using X-ray fluorescence analysis (XRF, Epsilon5, PANalytical, Netherlands) on Teflon filters before acid digestion. The QA/QC procedures of the XRF analysis have been described in Xu et al. (2012a).

The other half of all filter samples was used for extraction with 20 mL ultrapure water (specific resistivity = 18.2 MΩ cm; Millipore, Massachusetts, United States) for 1 h. Analysis of extract solutions was performed with an ion chromatograph (Dionex ICS-900 and ICS-1100) equipped with a conductivity detector (ASRS-ULTRA). A Dionex AS11-HC separator column was used for analyzing F<sup>-</sup>, Cl<sup>-</sup>, NO<sub>3</sub><sup>-</sup>, and SO<sub>4</sub><sup>2-</sup>. A CS12A separator column was used to analyze Na<sup>+</sup>, NH<sub>4</sub><sup>+</sup>, K<sup>+</sup>, Mg<sup>2+</sup>, and Ca<sup>2+</sup>. The eluents used were 22 to 25 mM for anions and 20 mM methansulfonic acid (MSA) for cations. In general, method detection limits (MDL) were within the range of 0.01 to 0.04 μg m<sup>-3</sup> for cations and 0.03 to 0.07 μg m<sup>-3</sup> for anions (Hsu et al., 2007).

#### 2.4.3 Sugar measurements

A 2.0 cm<sup>2</sup> punch from each quartz filter was extracted in 2 mL of ultrapure water under ultrasonic agitation for 1 h. Ex-

tracts were filtered through a syringe filter (pore size 0.25 μm, PTFE, Whatman, USA) to remove insoluble materials. Anhydrosugar levoglucosan (LG) and mannosan (MN) were measured by a Dionex ICS-3000 system. Instrumental controls, data acquisition, and chromatographic integration were performed using Dionex Chromeleon software. A calibration was performed for each analytical sequence. The DL for LG and MN were 0.002 mg L<sup>-1</sup>. A detailed description of the analytical method can be found elsewhere (Tao et al., 2013; Engling et al., 2006; Iinuma et al., 2009).

#### 2.5 Measurements of meteorological parameters

Meteorological parameters including wind direction, wind speed, relative humidity (RH), temperature, and precipitation were measured every 10 min. Wind direction and wind speed were recorded by a wind monitor (Vaisala Company, Helsinki, Finland, model QMW101). Ambient RH and temperature were measured by an RH/temperature probe (Vaisala Company, Helsinki, Finland, model QMH101). Precipitation was measured using a rain gauge (Vaisala Company, Helsinki, Finland, model QMR101). Both meteorological instruments were mounted at 3 m above the roof of the CRAES building (24 m above ground). Solar radiation data were obtained from a national meteorological station (30.7° N, 103.8° E) located 20 km from CRAES.

#### 2.6 Data analysis methods

To analyze chemical mass closure of PM<sub>2.5</sub>, PM<sub>2.5</sub> mass was reconstructed as the sum of organic matter (OM), EC, inorganic ions, water content, fine soil (FS), and trace element oxides (TEO). The factor converting OC to OM was 1.6 for spring and summer, and 1.8 for autumn and winter, as explained in Sect. 3.1.2. Water content was calculated using the thermodynamic equilibrium model ISORROPIA II (reserve mode) (Fountoukis and Nenes, 2007). To evaluate the model performance, statistical metrics including mean bias (MB), normalized mean bias (NMB), normalized mean error (NME) and the root-mean-square error (RMSE) were calculated as below (Eder and Yu., 2006):

$$\text{MB} = \frac{1}{N} \sum_1^N (C_m - C_o), \quad (1)$$

$$\text{NMB} = \frac{\sum_1^N (C_m - C_o)}{\sum_1^N C_o} 100\%, \quad (2)$$

$$\text{NME} = \frac{\sum_1^N |C_m - C_o|}{\sum_1^N C_o} 100\%, \quad (3)$$

$$\text{RMSE} = \sqrt{\frac{1}{N} \sum_1^N (C_m - C_o)^2}, \quad (4)$$

where  $C_m$  and  $C_o$  are modeled and observed concentration of total inorganic ions, respectively.

The FS component was estimated using the following formula (Malm et al., 1994):

$$[\text{FS}] = 2.20[\text{Al}] + 2.49[\text{Si}] + 1.63[\text{Ca}] + 2.42[\text{Fe}] + 1.94[\text{Ti}]. \quad (5)$$

However, Si is mostly volatilized as SiF<sub>4</sub> in acid digestion when using HF. Thus, we used Si data analyzed by XRF, whereas the data for other four elements were obtained from ICP-MS measurement.

For TEO, the contribution of heavy metals as metal oxides was estimated using the following equation (Zhang et al., 2013):

$$\begin{aligned} \text{TEO} = & 1.3 \times [0.5 \times (\text{Sr} + \text{Ba} + \text{Mn} + \text{Co} + \text{Rb} + \text{Ni} + \text{V}) \\ & + 1.0 \times (\text{Cu} + \text{Zn} + \text{Mo} + \text{Cd} + \text{Sn} + \text{Sb} + \text{Tl} + \text{Pb} \\ & + \text{As} + \text{Se} + \text{Ge} + \text{Cs} + \text{Ga})]. \quad (6) \end{aligned}$$

Source apportionment analysis was conducted using positive matrix factorization (PMF) model version 3.0 of the Environmental Protection Agency (EPA), US (Norris et al., 2008). To reduce uncertainties of PMF results, chemical components with annual average concentrations below MDLs were removed, such as F<sup>-</sup> and REEs, which are essentially similar to the major crustal elements such as Al. Thirty-five chemical components were used for the PMF model, including OC, EC, LG, Na<sup>+</sup>, NH<sub>4</sub><sup>+</sup>, K<sup>+</sup>, Mg<sup>2+</sup>, Ca<sup>2+</sup>, Cl<sup>-</sup>, NO<sub>3</sub><sup>-</sup>, SO<sub>4</sub><sup>2-</sup>, Al, Fe, Mg, Ca, Sr, Ba, Ti, Mn, Ni, Cu, Zn, Mo, Cd, Sn, Sb, Tl, Pb, V, Cr, As, Se, Zr, Ge, Rb, Cs, and Ga. To determine the appropriate number of source factors, a reasonable practice is to test different numbers of identifiable sources commonly used and to consider the major potential sources documented by the local Environmental Protection Bureau. In this study, we have tested five, six, seven, and even eight different sources in the PMF analysis. Then, PMF was run several times with different  $F_{\text{peak}}$  values to determine the range within which the objective function  $Q$  values remains relatively constant (Supplement Fig. S2). In the six-factor model, a value of  $F_{\text{peak}} = -0.1$  provided the most physically reasonable source profiles.

Three-day backward trajectories were calculated at an elevation of 500 and 1500 m for every sampling day starting at 02:00 UTC (10:00 LT) using the HYbrid Single-Particle Lagrangian Integrated Trajectory (HYSPPLIT) 4 trajectory model (<http://ready.arl.noaa.gov/HYSPLIT.php>) to investigate synoptic patterns and transport routes of air masses (Draxler and Rolph, 2013; Rolph, 2013). The model adopted meteorological data from FNL (final operational global analysis) as input.

### 3 Results and discussion

#### 3.1 General characteristics of PM<sub>2.5</sub> and chemical components

The annual average of PM<sub>2.5</sub> mass concentrations in Chengdu was  $119 \pm 56 \mu\text{g m}^{-3}$  (Table 1), which was 3 times

higher than the NAAQS for annual PM<sub>2.5</sub> ( $35 \mu\text{g m}^{-3}$ ). As summarized in Table 1, the PM<sub>2.5</sub> level in Chengdu was only significantly lower than that for one inland megacity, Xi'an ( $194 \mu\text{g m}^{-3}$ ), located in northwest China (Zhang et al., 2011), and was comparable with the other two megacities – Chongqing (Yang et al., 2011), also located in the Sichuan Basin, and Beijing (Zhang et al., 2013). However, PM<sub>2.5</sub> in Chengdu was much higher than those observed in coastal megacities, such as Tianjin (Gu et al., 2010), Shenyang (Ma et al., 2011), Shanghai (Feng et al., 2009), Fuzhou (Xu et al., 2012b), Xiamen (Zhang et al., 2012), Guangzhou (Tao et al., 2014), and Hong Kong (Louie et al., 2005). The annual average PM<sub>2.5</sub> in Chengdu was higher by a factor of 3 to 15 compared with those in other developed countries (Balasubramanian et al., 2003; Heo et al., 2009; Khan et al., 2009; Pinto et al., 2004; Querol et al., 2004). Thus, Chengdu is suffering from a considerably severe PM<sub>2.5</sub> pollution problem in the world.

A typical seasonal variation in PM<sub>2.5</sub> mass concentrations was observed (Table 2), with higher concentrations in winter ( $158 \mu\text{g m}^{-3}$ ) and spring ( $126 \mu\text{g m}^{-3}$ ) and lower concentrations in autumn ( $111 \mu\text{g m}^{-3}$ ) and summer ( $89 \mu\text{g m}^{-3}$ ). Generally, PM<sub>2.5</sub> levels are governed by emissions, transportation, chemical transformation, and depositional processes, which are all related to meteorological conditions. However, systematic investigations on PM<sub>2.5</sub> emission inventories have not been conducted in Sichuan (including Chengdu). The highest wintertime PM<sub>2.5</sub> concentration could be partly related to certain weather conditions in terms of low mixing height because of weak solar radiation (Supplement Fig. S3). By contrast, the lowest summertime concentration was in part due to frequent rainfall (Supplement Fig. S3), which led to efficient removal of suspended particles from the atmosphere (Wang et al., 2010).

#### 3.1.1 Carbonaceous aerosols and biomass burning markers

Annual mean concentrations of OC and EC were  $17 \pm 8$  and  $7 \pm 4 \mu\text{g m}^{-3}$ , accounting for PM<sub>2.5</sub> masses of  $14.3 \pm 4.4$  and  $5.7 \pm 1.5\%$ , respectively (Table 2). Seasonal variation of EC was similar to that of PM<sub>2.5</sub>, following the order of winter ( $8 \pm 8 \mu\text{g m}^{-3}$ ) > spring ( $7 \pm 5 \mu\text{g m}^{-3}$ ) ≥ autumn ( $7 \pm 3 \mu\text{g m}^{-3}$ ) > summer ( $6 \pm 3 \mu\text{g m}^{-3}$ ). However, the seasonal pattern of OC was somewhat different from those of EC and PM<sub>2.5</sub>, with the second highest season in autumn ( $20 \pm 9 \mu\text{g m}^{-3}$ ) instead of in spring ( $15 \pm 7 \mu\text{g m}^{-3}$ ). The distinct seasonality between OC and EC implies likely changes in the strength of their respective sources in different seasons. LG concentrations were nearly identical in autumn ( $659 \pm 441 \text{ ng m}^{-3}$ ) and winter ( $635 \pm 246 \text{ ng m}^{-3}$ ), followed by spring ( $235 \pm 151 \text{ ng m}^{-3}$ ) and summer ( $152 \pm 89 \text{ ng m}^{-3}$ ), with an annual mean of  $412 \pm 352 \text{ ng m}^{-3}$ . However, MN showed a more typical seasonality compared with LG, with a

**Table 1.** Statistics of annual PM<sub>2.5</sub> mass concentrations in urban Chengdu and other cities in the world.

City/nation	Sampling period	PM <sub>2.5</sub> (µg m <sup>-3</sup> )	Reference
Chengdu, southwest China	2011	119	This study
Chongqing, southwest China	2005–2006	129.0	Yang et al. (2011)
Xi'an, northwest China	2009	194.1	Zhang et al. (2011)
Beijing, north China	2009–2010	135.0	Zhang et al. (2013)
Tianjin, north China	2008	109.8	Gu et al. (2010)
Shenyang, northeast China	2006–2008	75	Ma et al. (2011)
Shanghai, east China	2005–2006	90.3	Feng et al. (2009)
Fuzhou, southeast China	2007–2008	44.33	Xu et al. (2012b)
Xiamen, southeast China	2009–2010	86.16	Zhang et al. (2012)
Guangzhou, south China	2009–2010	76.0	Tao et al. (2014)
Hong Kong, south China	2000–2001	56.7	Louie et al. (2005)
Seoul, Korea	2003–2006	43.5	Heo et al. (2009)
Yokohama, Japan	2007–2008	20.6	Khan et al. (2009)
Singapore, Singapore	2000	27.2	Balasubramanian et al. (2003)
27 urban sites, US	1999–2000	<35	Pinto et al. (2004)
Austria; Germany; Switzerland; Netherlands; UK (central Europe)	1998–2002	16–30	Querol et al. (2004)
Sweden (northern Europe)	1998–2002	8–15	Querol et al. (2004)
Spain (southern Europe)	1998–2002	19–25	Querol et al. (2004)

maximum ( $80 \pm 34 \text{ ng m}^{-3}$ ) in winter, followed by autumn ( $36 \pm 27 \text{ ng m}^{-3}$ ), spring ( $19 \pm 17 \text{ ng m}^{-3}$ ), and summer ( $9 \pm 7 \text{ ng m}^{-3}$ ). The levels of these two markers were much higher than those measured in European countries such as Sweden (Szidat et al., 2009), Belgium (Zdráhal et al., 2002), Switzerland (Szidat et al., 2006), and Norway (Yttri et al., 2009).

Sources of carbonaceous aerosols can be further qualitatively evaluated by the relationship of OC against EC (Turpin and Huntzicker, 1995) and biomass burning markers against OC or EC (Szidat et al., 2009). For instance, large discrepancies and variability in OC/EC ratios reportedly exist in coal combustion (0.3–7.6), vehicle emission (0.7–2.4), and biomass burning (4.1–14.5) (Watson et al., 2001). As shown in Fig. 2a, OC and EC in Chengdu were well correlated in each season, with an  $R^2$  ranging from 0.65 to 0.85. Mean OC/EC ratios increased from 2.0 in spring and 1.8 in summer to 2.9 in autumn and 2.6 in winter. These average ratios were lower than those (3.3) measured in PM<sub>10</sub> in Chengdu in 2006, but within the range found across China by Zhang et al. (2008a). Good correlations between OC and EC, but distinct OC/EC ratios suggest that OC and EC were derived from similar sources that varied seasonally. As depicted in Fig. 2b and 2c, LG correlated with OC and MN, with the LG/OC ratio ranging from 0.015 in summer to 0.034 in winter and the LG/MN ratios ranging from 7.8 in winter to 17 in autumn. In addition to the differences in seasonal ratios, correlations were also quite variable from season to season, with the highest coefficient ( $R^2 \geq 0.90$ ) in winter and the lowest ( $R^2 < 0.60$ ) in summer. Again, features of biomass

burning biomarker revealed that biomass burning sources of carbonaceous aerosols varied with the season. The LG/OC ratio has been applied as a tracer of wood burning (Szidat et al., 2009, and references therein), whereas LG/MN ratio has been used for distinguishing specific types of biomass burning (Engling et al., 2009). A relatively high LG/OC ratio (0.029) and low LG/MN ratio (7.8) in winter compared to those in spring and summer may indicate dominance of wood burning (Szidat et al., 2009; Oliveira et al., 2007; Pio et al., 2008). By contrast, the highest LG/OC (0.034) and LG/MN (17) ratios in autumn over the sampling year could reveal combined sources of wood burning together with rice straw and other agricultural residue burning (Sheesley et al., 2003; Engling et al., 2009). These suggestions are in agreement with the fact that residents in the Sichuan Basin used to utilize woods as energy source to generate heat in cold winters (Edwards et al., 2004; Yan et al., 2006). In addition to residential use, waste wood was used by nearly 1000 smaller coal boilers (less than  $10 \text{ t vapor h}^{-1}$ ). Agricultural waste burning was usually most severe in harvest season – autumn – in China (Duan et al., 2004). Our LG/OC ratios were much lower than those ( $\sim 0.135$ ) typically detected in wood burning (Szidat et al., 2009, and references therein) as OC was produced from additional sources besides biomass burning. Using the mean concentration of LG (Table 2) divided by this characteristic ratio (none was available in China), we estimated an annual contribution of  $3.1 \text{ µg m}^{-3}$  (varying from 1.1 to  $4.9 \text{ µg m}^{-3}$  in the four seasons) from wood burning, which represents 18% of the observed total OC (ranging from 11 to 24% in varying seasons)

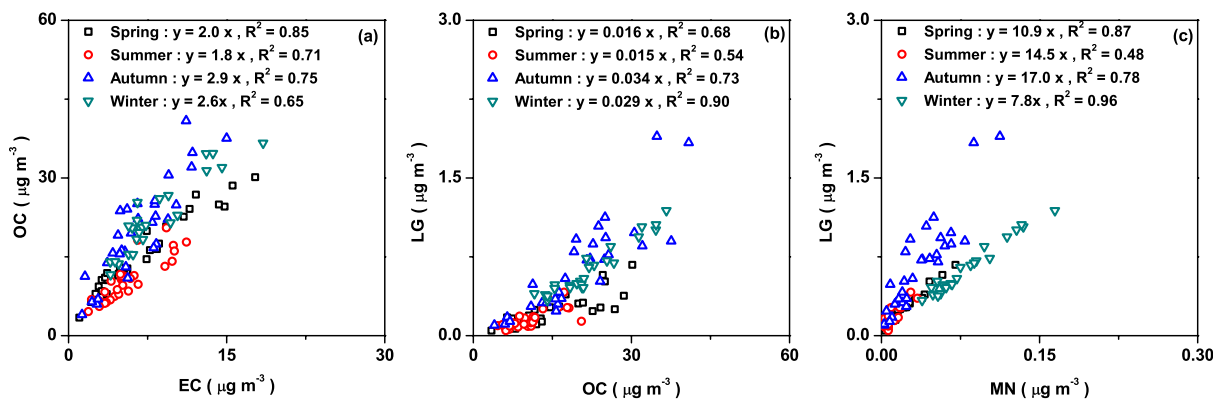


**Figure 2.** Scatter plots of OC vs. EC (a), LG vs. OC (b), and LG vs. MN (c) in four seasons. Also shown are the linear regression lines with regression equations.

in Chengdu. The annual mean proportion is lower than that ( $\sim 30\%$ ) acquired from PMF modeling, which is presented below. This finding indicates that biomass burning other than wood burning sources (e.g., agricultural waste burning) accounted for the rest of the contributions (i.e.,  $\sim 10\%$ ) to the OC.

Lei et al. (2011) reported that the 2005 primary OC and EC emissions from anthropogenic sources in China were 1.51 and 3.19 Tg, respectively. In Sichuan province, the residential sector was the largest contributor, constituting 47% to black carbon (BC) and 81% to OC. In other regions of China, the dominant sector could be different (Cao et al., 2006; Zhao et al., 2012). For example, the industrial sector is dominant in northern China provinces such as Hebei, Shanxi, Shandong, and Henan. According to Qin and Xie (2012), annual BC emission from Sichuan in 2009 has increased to over 0.14 Tg. Coal was still the most predominant fuel used in China, which alone contributed nearly 50% to the national BC emission (Qin and Xie, 2012). Based on the coincidence of OC/EC ratios between the PM<sub>2.5</sub> aerosols (annual mean  $\sim 2.4$ ) and emissions ( $\sim 2.1$ ), coal combustion appeared to be an important source of carbonaceous aerosols throughout the year. The factor converting OC to OM has been suggested to vary with its dominant sources and the age of organic aerosols (Turpin and Lim, 2001; Andreae and Rosenfeld, 2008). In the present study, a value of 1.6 was adopted for spring and summer, and 1.8 for autumn and winter. These values were consistent with those recently observed across China (Xing et al., 2013), although slightly lower than those found across the US, which had a median value of 1.80 to 1.95 (Simon et al., 2011).

### 3.1.2 Water-soluble ions

Water-soluble ions also comprised important constituents of PM<sub>2.5</sub>. The sum of all the major water-soluble ions averaged  $52 \pm 29 \mu\text{g m}^{-3}$  in Chengdu (Table 2), accounting for  $42 \pm 9\%$  of PM<sub>2.5</sub> mass.  $\text{SO}_4^{2-}$ ,  $\text{NO}_3^-$ , and  $\text{NH}_4^+$  were the

dominant ions, and their combination constituted  $90 \pm 5\%$  of total ion concentrations. To investigate the associations among ions, a thermodynamic equilibrium model, ISORROPIA II (Fountoukis and Nenes, 2007), was applied to simulate chemical components and phase state of major ions in thermodynamic equilibrium conditions. Water and inorganic salt concentrations were simultaneously estimated by ISORROPIA II model (reserve mode) at a fixed relative humidity (RH 40%) and temperature (23 °C). Seven compounds that had concentrations larger than zero were derived (Table 3). On annual average, the total concentrations of all inorganic chemical species calculated by ISORROPIA II model was  $51 \pm 28 \mu\text{g m}^{-3}$ , which was very close to the sum of all the observed ions concentrations ( $52 \pm 29 \mu\text{g m}^{-3}$ ). To evaluate ISORROPIA II model performances, the statistical parameters MB, NMB, NME, and RMSE for total ion concentrations were calculated by Eqs. (1)–(4). The MB, NMB, NME, and RMSE values are  $-1.2$ ,  $-2.3$ ,  $2.3$ , and  $1.6\%$ , suggesting that the ISORROPIA II model can reasonably simulate most of the observed ions. Both  $\text{SO}_4^{2-}$  and  $\text{NO}_3^-$  were mostly associated with  $\text{NH}_4^+$ , present in the forms of  $(\text{NH}_4)_2\text{SO}_4$  and  $\text{NH}_4\text{NO}_3$ . All  $\text{Cl}^-$  were exclusively present in the form of  $\text{NH}_4\text{Cl}$ . Besides  $\text{NH}_4^+$ , the other four cations ( $\text{K}^+$ ,  $\text{Na}^+$ ,  $\text{Ca}^{2+}$ , and  $\text{Mg}^{2+}$ ) were also associated with  $\text{SO}_4^{2-}$ . Seasonal variations in concentrations of the predominant chemical species,  $(\text{NH}_4)_2\text{SO}_4$  and  $\text{NH}_4\text{NO}_3$ , were consistent with those of  $\text{SO}_4^{2-}$  and  $\text{NO}_3^-$  concentrations that showed the highest concentrations in winter and the lowest in summer or autumn (Table 2). Liquid water derived by the ISORROPIA II model reached  $15.0 \pm 8.4 \mu\text{g m}^{-3}$  on the average, following similar seasonal patterns of major ions.

### 3.1.3 Metal elements

Daily concentrations of FS and TEO were calculated using Eqs. (5) and (6). Annual concentrations of FS and TEO were  $6.7 \pm 4.4$  and  $1.1 \pm 0.6 \mu\text{g m}^{-3}$ , which accounted for  $6.3 \pm 4.8$  and  $0.9 \pm 0.3\%$ , respectively, of PM<sub>2.5</sub> mass.

**Table 2.** Statistics of PM<sub>2.5</sub> chemical components in four seasons.

	Annual ( <i>n</i> = 117)	Spring ( <i>n</i> = 31)	Summer ( <i>n</i> = 30)	Autumn ( <i>n</i> = 31)	Winter ( <i>n</i> = 25)
PM <sub>2.5</sub> /μg m <sup>-3</sup>	119 ± 56	126 ± 66	89 ± 35	111 ± 49	158 ± 51
OC/μg m <sup>-3</sup>	17 ± 8	15 ± 7	11 ± 4	20 ± 9	22 ± 7
EC/μg m <sup>-3</sup>	7 ± 4	7 ± 5	6 ± 3	7 ± 3	8 ± 4
Na <sup>+</sup> /μg m <sup>-3</sup>	0.6 ± 0.3	0.7 ± 0.3	0.5 ± 0.2	0.5 ± 0.3	0.5 ± 0.2
NH <sub>4</sub> <sup>+</sup> /μg m <sup>-3</sup>	11.6 ± 7.3	11.9 ± 10.0	9.0 ± 5.0	11.1 ± 6.0	15.3 ± 5.7
K <sup>+</sup> /μg m <sup>-3</sup>	1.7 ± 0.8	1.5 ± 0.8	1.3 ± 0.6	1.8 ± 0.7	2.1 ± 0.7
Mg <sup>2+</sup> /μg m <sup>-3</sup>	0.1 ± 0.0	0.1 ± 0.1	0.1 ± 0.0	0.0 ± 0.0	0.1 ± 0.0
Ca <sup>2+</sup> /μg m <sup>-3</sup>	0.4 ± 0.3	0.6 ± 0.4	0.3 ± 0.2	0.3 ± 0.1	0.3 ± 0.1
F <sup>-</sup> /μg m <sup>-3</sup>	0.1 ± 0.1	0.1 ± 0.1	0.0 ± 0.0	0.1 ± 0.1	0.1 ± 0.0
Cl <sup>-</sup> /μg m <sup>-3</sup>	1.7 ± 1.7	1.5 ± 1.5	0.4 ± 0.4	2.5 ± 1.6	2.8 ± 1.9
NO <sub>3</sub> <sup>-</sup> /μg m <sup>-3</sup>	10.7 ± 7.8	10.2 ± 8.7	5.3 ± 3.2	12.9 ± 8.5	15.5 ± 5.4
SO <sub>4</sub> <sup>2-</sup> /μg m <sup>-3</sup>	25.0 ± 14.1	26.4 ± 18.1	23.7 ± 13.5	19.2 ± 9.6	31.8 ± 10.7
LG/ng m <sup>-3</sup>	412 ± 352	235 ± 151	152 ± 89	659 ± 441	635 ± 246
MN/ng m <sup>-3</sup>	34 ± 35	19 ± 17	9 ± 7	36 ± 27	80 ± 34
Al/ng m <sup>-3</sup>	560 ± 420	898 ± 581	427 ± 331	462 ± 217	426 ± 201
Fe/ng m <sup>-3</sup>	693 ± 420	899 ± 561	610 ± 363	640 ± 303	606 ± 335
Na/ng m <sup>-3</sup>	837 ± 680	865 ± 413	736 ± 342	847 ± 344	658 ± 283
Mg/ng m <sup>-3</sup>	196 ± 164	299 ± 251	147 ± 123	166 ± 78	164 ± 86
K/ng m <sup>-3</sup>	1576 ± 751	1575 ± 876	1312 ± 623	1757 ± 777	1681 ± 640
Ca/ng m <sup>-3</sup>	402 ± 339	588 ± 440	341 ± 344	389 ± 218	262 ± 203
Sr/ng m <sup>-3</sup>	5.7 ± 4.1	7.5 ± 4.9	3.6 ± 2.5	5.4 ± 3.1	6.6 ± 4.6
Ba/ng m <sup>-3</sup>	22 ± 17	26 ± 13	13 ± 6	23 ± 15	30 ± 24
Ti/ng m <sup>-3</sup>	50 ± 33	71 ± 43	46 ± 32	47 ± 23	35 ± 17
Mn/ng m <sup>-3</sup>	66 ± 37	78 ± 51	59 ± 28	63 ± 32	65 ± 28
Ni/ng m <sup>-3</sup>	2.5 ± 1.6	2.5 ± 1.4	2.0 ± 0.8	2.6 ± 1.5	3.2 ± 2.3
Cu/ng m <sup>-3</sup>	23 ± 12	26 ± 15	23 ± 10	18 ± 10	27 ± 12
Zn/ng m <sup>-3</sup>	350 ± 230	440 ± 318	324 ± 182	310 ± 164	319 ± 205
Mo/ng m <sup>-3</sup>	3.8 ± 3.8	2.6 ± 1.7	2.7 ± 1.5	4.6 ± 4.3	5.4 ± 5.8
Cd/ng m <sup>-3</sup>	3.5 ± 1.9	4.1 ± 2.4	3.1 ± 1.5	3.0 ± 1.6	4.0 ± 2.0
Sn/ng m <sup>-3</sup>	10.6 ± 6.9	12.7 ± 9.3	9.0 ± 4.7	9.7 ± 5.9	11.0 ± 6.6
Sb/ng m <sup>-3</sup>	6.5 ± 4.2	8.2 ± 5.5	4.8 ± 2.4	5.2 ± 2.9	8.1 ± 4.3
Tl/ng m <sup>-3</sup>	1.9 ± 1.1	2.5 ± 1.6	1.4 ± 0.4	1.6 ± 0.8	2.3 ± 1.1
Pb/ng m <sup>-3</sup>	172 ± 86	198 ± 107	142 ± 58	154 ± 68	198 ± 94
V/ng m <sup>-3</sup>	1.7 ± 0.9	2.2 ± 1.2	1.4 ± 0.7	1.6 ± 0.7	1.6 ± 0.6
Cr/ng m <sup>-3</sup>	9.2 ± 5.0	10.0 ± 6.4	9.7 ± 3.8	8.6 ± 5.0	8.3 ± 4.2
As/ng m <sup>-3</sup>	20 ± 11	19 ± 12	21 ± 12	22 ± 10	18 ± 10
Se/ng m <sup>-3</sup>	2.7 ± 1.2	2.9 ± 1.6	2.3 ± 0.7	2.9 ± 1.3	2.9 ± 1.0
Zr/ng m <sup>-3</sup>	2.8 ± 1.6	4.0 ± 1.9	2.3 ± 1.2	2.5 ± 1.3	2.4 ± 1.2
Ge/ng m <sup>-3</sup>	1.1 ± 0.6	1.2 ± 0.7	0.9 ± 0.3	1.0 ± 0.5	1.2 ± 0.5
Rb/ng m <sup>-3</sup>	7.6 ± 3.7	8.6 ± 5.0	6.6 ± 2.7	7.2 ± 3.2	8.2 ± 3.0
Cs/ng m <sup>-3</sup>	1.2 ± 0.6	1.1 ± 0.7	1.2 ± 0.6	1.3 ± 0.7	1.2 ± 0.5
Ga/ng m <sup>-3</sup>	5.8 ± 3.1	5.9 ± 3.5	5.1 ± 2.1	6.3 ± 3.5	5.8 ± 3.1
Si*/ng m <sup>-3</sup>	1204 ± 860	1962 ± 1142	933 ± 719	868 ± 392	1020 ± 351

\* Si analysis by XRF method.

Seasonal concentrations of FS decreased from 10.1 μg m<sup>-3</sup> in spring to 5.5 μg m<sup>-3</sup> in autumn and 5.4 μg m<sup>-3</sup> in winter and summer. For TEO, seasonal variability was relatively small, declining from 1.3 μg m<sup>-3</sup> in spring to 1.1 μg m<sup>-3</sup> in winter, 1.0 μg m<sup>-3</sup> in autumn, and 0.9 μg m<sup>-3</sup> in summer.

Both FS and TEO concentrations similarly waxed in spring, with small fluctuations seen in the other seasons.

The total concentration of all the trace metals (i.e., excluding Al, Fe, Na, Mg, K, and Ca) was 0.8 ± 0.4 μg m<sup>-3</sup>, constituting 0.7 ± 0.3 % of PM<sub>2.5</sub> mass. As, Cd, Co, Cr, Ni, Pb,

**Table 3.** The calculated chemical components and phase state of ions ( $\mu\text{g m}^{-3}$ ) in lab condition (temp: 23 °C; RH: 40 %) in Chengdu. Results were modeled by the ISORROPIA II.

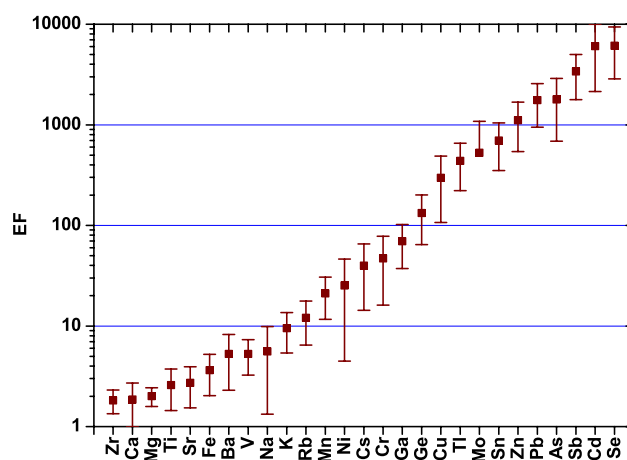
	Annual ( <i>n</i> = 117)	Spring ( <i>n</i> = 31)	Summer ( <i>n</i> = 30)	Autumn ( <i>n</i> = 31)	Winter ( <i>n</i> = 25)
(NH <sub>4</sub> ) <sub>2</sub> SO <sub>4</sub>	28.3 ± 18.1	29.2 ± 23.1	27.5 ± 17.6	20.7 ± 12.0	37.4 ± 13.8
Na <sub>2</sub> SO <sub>4</sub>	1.8 ± 0.9	2.2 ± 1.0	1.6 ± 0.7	1.7 ± 0.8	1.6 ± 0.7
K <sub>2</sub> SO <sub>4</sub>	3.8 ± 1.7	3.4 ± 1.9	3.0 ± 1.3	4.1 ± 1.7	4.7 ± 1.6
MgSO <sub>4</sub>	0.3 ± 0.2	0.5 ± 0.4	0.3 ± 0.2	0.2 ± 0.1	0.4 ± 0.2
CaSO <sub>4</sub>	1.2 ± 0.9	2.0 ± 1.3	0.9 ± 0.7	0.9 ± 0.5	1.0 ± 0.4
NH <sub>4</sub> NO <sub>3</sub>	13.5 ± 10.3	12.8 ± 11.3	5.9 ± 4.3	16.7 ± 10.9	19.6 ± 7.3
NH <sub>4</sub> Cl	1.9 ± 2.5	1.6 ± 2.4	0.3 ± 0.4	3.7 ± 2.3	2.1 ± 2.7
H <sub>2</sub> O(aq)	15.0 ± 8.4	15.3 ± 10.6	12.4 ± 6.9	13.1 ± 6.8	19.8 ± 6.9
Σ species	64.2 ± 36.4	66.7 ± 46.9	50.9 ± 27.3	58.2 ± 30.9	84.7 ± 29.3
Σ species/PM <sub>2.5</sub> (%)	54.8 ± 16.1	51.2 ± 14.6	61.7 ± 20.6	51.2 ± 16.0	55.3 ± 6.7

and Se are well-known carcinogenic heavy metals registered in the US Agency for Toxic Substances and Disease Registry. Noticeably, the annual mean concentration of As in Chengdu exceeded the WHO standard ( $6.6 \text{ ng m}^{-3}$ , lifetime risk level is 1 : 100 000) by a factor of 3 (World Health Organization, 2000). Twenty-five of the 117 samples exceeded  $5 \text{ ng m}^{-3}$  Cd concentration, which is the WHO's guide value (World Health Organization, 2000).

Enrichment factors (EFs) relative to the Earth's upper crust composition can be used for assessing the anomaly of elemental composition of aerosol particles. In this study, Al served as a reference element. The average composition of Earth's crust was referenced from Hans Wedepohl (1995). The EFs of Zr, Ca, Mg, Ti, Sr, Fe, Ba, V, Na, and K were less than 10; EFs of Rb, Mn, Ni, Cs, Cr, Ga, and Ge ranged from 10 to 100; and EFs of Cu, Tl, Mo, Sn, Zn, Pb, As, Sb, Cd, and Se were larger than 100 (Fig. 3). The EFs of carcinogenic heavy metals, As, Cd, Co, Cr, Ni, Pb, and Se were  $1772 \pm 1091$ ,  $6060 \pm 3942$ ,  $6 \pm 5$ ,  $47 \pm 31$ ,  $25 \pm 21$ ,  $1753 \pm 814$ , and  $6095 \pm 3261$ , respectively, indicating that these heavy metals were of anthropogenic origins, except for Co, which was further analyzed below by the PMF results. Therefore, carcinogenic heavy metal pollution, especially As, in Chengdu was serious. Control strategies must be undertaken to alleviate heavy metal loadings.

### 3.2 Reconstructed PM<sub>2.5</sub> mass

The PM<sub>2.5</sub> mass in Chengdu was reconstructed on seasonal and annual basis by employing the methods described in Sect. 2.6. PM<sub>2.5</sub> mass concentrations could be reconstructed by combining the main components, as depicted in Fig. 4. The correlations ( $R^2$ ) between the reconstructed and measured mass concentrations were higher than 0.93 in all the seasons and the seasonal average mass ratio ranged from 0.90 to 0.99. On average, the reconstructed masses explained  $92 \pm 11 \%$  of measured ones, indicating a good performance of the formulations applied. Based on the results, PM<sub>2.5</sub>

**Figure 3.** Enrichment factors of trace elements.

in the urban area of Chengdu was composed of OM, EC, FS, TEO, inorganic ions, and water, with contributions of  $24.5 \pm 8.4$ ,  $5.7 \pm 1.5$ ,  $6.3 \pm 4.8$ ,  $0.9 \pm 0.3$ ,  $42.2 \pm 9.0$ , and  $12.2 \pm 3.0 \%$ , respectively.

As illustrated in Fig. 5, the total of inorganic ions was the largest contributor to PM<sub>2.5</sub>, accounting for a relatively constant fraction of 40 to 44 % in the four seasons. Also, contributions of EC, TEO, and water to PM<sub>2.5</sub> were relatively constant from season to season. However, seasonal variations were evident for the contributions of OM and FS to PM<sub>2.5</sub>, with OM contributed 19.4, 19.8, 33.4, and 25.6 % in spring, summer, autumn, and winter, respectively, and FS contributed 9.3, 6.4, 5.3, and 3.7 %, respectively. Fig. 2a and b show relatively higher OC / EC ratios (2.9 and 2.6, respectively) and better correlations ( $R^2 = 0.73$  and 0.90, respectively) between biomass burning tracer LG and OC in autumn and winter, demonstrating more OM contributed from biomass burning in autumn and winter. Because PM<sub>2.5</sub> concentrations were lower in summer than those in autumn and winter, the resulting contribution of FS to PM<sub>2.5</sub> was

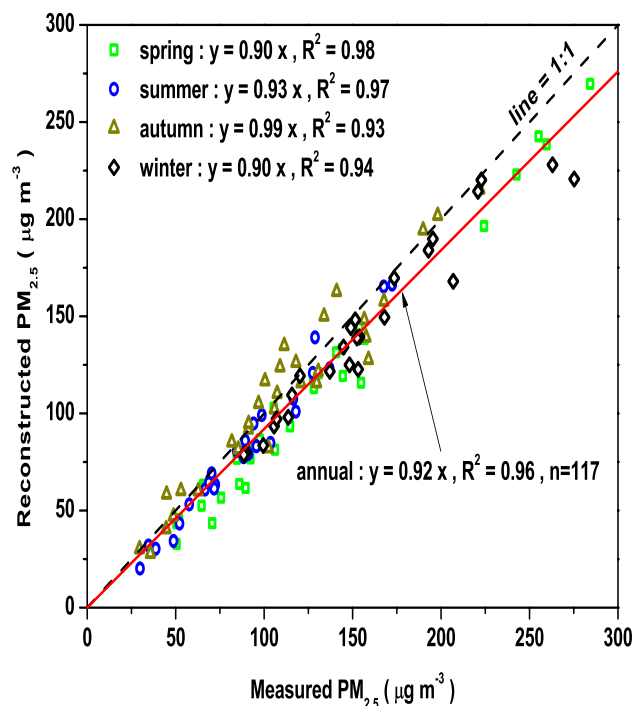


**Figure 4.** Correlation between reconstructed and measured PM<sub>2.5</sub> mass concentrations in four seasons. Also shown are the linear regression lines with regression equations.

relatively higher in summer than those in autumn and winter. These results suggest that biomass burning and soil dust had contrasting trends in contributing to PM<sub>2.5</sub>, with more OM contributions in autumn and winter and more dust contributions in spring and summer, which is also consistent with the PMF results, as discussed in the next section.

### 3.3 Source apportionment

Based on the PMF modeling results, six main source factors were identified, including secondary inorganic aerosols, coal combustion, biomass burning, the iron and steel industry, Mo-related industries, and soil dust. Modeled source profiles together with the relative contributions of individual sources to each analyzed species are shown in Fig. 6. Their contributions are summarized in Table 4. The annual and seasonal averages of the absolute ( $\mu\text{g m}^{-3}$ ) and fractional (%) contributions from each source were calculated based on their daily values simulated by PMF model. As expected, the annual averages of absolute and fractional contributions from identified sources, except the obvious seasonal sources – biomass burning and soil dust – are larger than their respective standard deviations. This suggests that the PMF results might be reasonable. To further confirm this assumption, the modeled time series of the contributions from each source was compared with the observed time series of certain chemical species that could represent respective sources (Fig. 7).

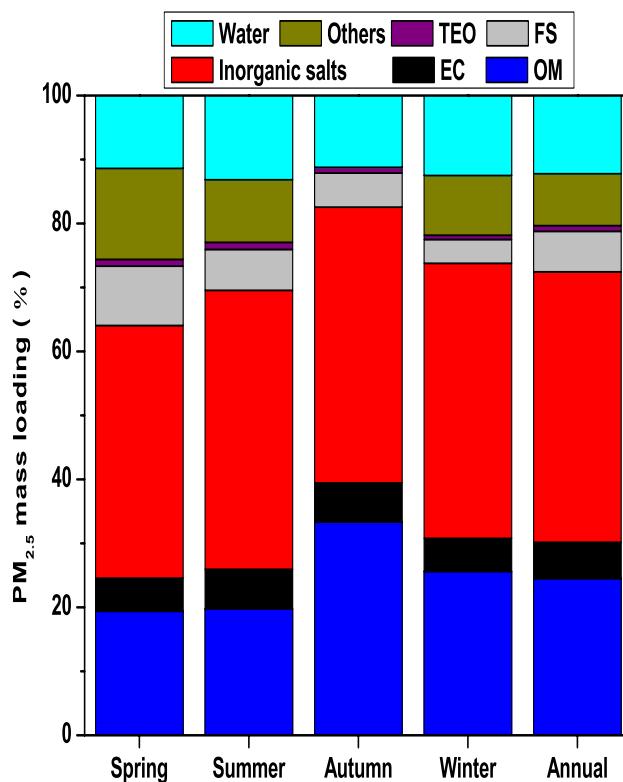


**Figure 5.** Chemical mass closures of PM<sub>2.5</sub> mass concentrations in four seasons. The major chemical components include inorganic salts, organic matter (OM), elemental carbon (EC), fine soil (FS), trace element oxides (TEO), and water content, as well as others that were unidentified.

The first source comprises secondary inorganic aerosols, characterized by high  $\text{NH}_4^+$ ,  $\text{SO}_4^{2-}$ , and  $\text{NO}_3^-$  concentrations (Fig. 6a) (Zhang et al., 2013). The PMF-derived secondary inorganic aerosols accounted for  $37 \pm 18\%$  of the PM<sub>2.5</sub> (Table 4). These secondary products were formed from the oxidation of main precursor gases, sulfur dioxide ( $\text{SO}_2$ ) and nitrogen oxides ( $\text{NO}_x$ ), that were mainly emitted from coal combustion, vehicle exhausts, and even biomass burning, which in turn interacted with ammonia ( $\text{NH}_3$ ) emitted mainly from agricultural activities and livestock waste. The ammonium ion is a typical secondary pollutant that is often a good tracer of secondary inorganic aerosols. As expected, temporal variations of secondary inorganic aerosol and  $\text{NH}_4^+$  concentrations were coincident (Fig. 7a), with an  $R^2$  of 0.76.

The second source is coal combustion, characterized by high EC, Zn, Cu, Sn, Sb, Tl, and Pb concentrations (Fig. 6b). This source represented a mean contribution of  $20 \pm 12\%$  to PM<sub>2.5</sub>, with a maximal absolute contribution ( $\sim 29 \mu\text{g m}^{-3}$ ) in spring and winter (Table 4), which agrees with the seasonal distribution of coal consumption in China. Coal combustion was the most dominant contributor of national  $\text{CO}_2$  emission in China, representing 72% (Gregg et al., 2008). In Sichuan, the main sources were industrial coal boilers and residential

**Table 4.** The contributions from six identified sources of PM<sub>2.5</sub> in Chengdu.

Sources	Annual		Spring		Summer		Autumn		Winter	
	$\mu\text{g m}^{-3}$	%								
Secondary inorganic aerosols	46 ± 32	37 ± 18	47 ± 37	37 ± 16	35 ± 24	37 ± 20	38 ± 28	33 ± 18	67 ± 29	44 ± 17
Coal combustion	22 ± 18	20 ± 12	29 ± 23	22 ± 12	20 ± 12	23 ± 12	13 ± 14	14 ± 13	29 ± 19	18 ± 9
Biomass burning	15 ± 17	11 ± 10	9 ± 9	7 ± 6	2 ± 4	1 ± 5	24 ± 17	19 ± 11	27 ± 17	16 ± 7
Iron and steel industry	13 ± 11	11 ± 9	12 ± 13	8 ± 7	16 ± 8	19 ± 9	13 ± 11	11 ± 8	8 ± 7	5 ± 4
Mo-related industries	12 ± 10	11 ± 9	8 ± 5	8 ± 5	7 ± 6	11 ± 14	15 ± 10	14 ± 7	20 ± 10	13 ± 5
Soil dust	10 ± 10	10 ± 12	18 ± 14	18 ± 17	8 ± 9	9 ± 12	8 ± 5	8 ± 7	4 ± 6	4 ± 5
Simulated PM <sub>2.5</sub> by PMF	118 ± 56	100	123 ± 68	100	88 ± 34	100	110 ± 49	100	155 ± 48	100
Measured PM <sub>2.5</sub>	119 ± 56		126 ± 66		89 ± 35		111 ± 49		158 ± 51	

coal stoves – the latter had significantly higher emissions of EC (Zhang et al., 2008b). Residential coal stoves were banned in Chengdu and thus smaller industrial coal boilers dominated this factor. Leaded gasoline has been banned since 2000 in China and coal combustion became the primary source of Pb aerosols in China. This source accounted for 31 % of the observed Pb in Chengdu (Fig. 6b) (Mukai et al., 2001). Dan et al. (2004) attributed the observed high Pb and Zn in wintertime PM<sub>2.5</sub> in Beijing to the coal combustion source. From a global perspective, coal combustion is the primary contributor of global emissions of Sb, Sn, and Tl in the atmosphere (Pacyna and Pacyna, 2001). According to a recent estimate, atmospheric Sb emission from China was up to 818 t per year, of which 61.8 % was emitted from coal combustion and the remaining 26.7 % was from nonferrous metal smelting (Tian et al., 2012). However, Sb was sometimes attributable to traffic emissions, particularly in urban areas (Sternbeck et al., 2002). For Sichuan, the quota of coal combustion in atmospheric Sb emission can reach 85 % (Tian et al., 2012). Based on our PMF results, coal combustion contributed 48 % of the observed Sb in Chengdu. As a consequence, PMF-derived time series of coal combustion contribution and our observed Sb show good covariation (Fig. 7b). This result further implies that Sb, at least in the Sichuan Basin, could be an effective tracer of coal combustion primary pollutants.

The third source factor is biomass burning, characterized by elevated OC, EC, LG, K<sup>+</sup>, NO<sub>3</sub><sup>-</sup>, and Cl<sup>-</sup> (Fig. 6c). This result can be corroborated by the results of Tao et al. (2013), which showed that significant amounts of OC, EC, LG, Cl<sup>-</sup>, and K<sup>+</sup> existed in local biomass burning smoke at a suburban site of Chengdu. LG has been demonstrated as a good tracer of biomass burning (Engling et al., 2009, and references therein). This factor accounted for 11 ± 10% of the PM<sub>2.5</sub> mass concentration. Contributions from this source factor to PM<sub>2.5</sub> were higher in autumn (19 ± 11 %) and winter (16 ± 7 %) than in spring (7 ± 6 %) and summer (1 ± 5 %) (Table 4), consistent with seasonal patterns of LG concentration. As expected, variation trends of biomass burning and LG mass concentrations were similar (Fig. 7) and a good correlation between them was found ( $R^2 = 0.77$ ). Notice-

ably, the LG concentration (235 ng m<sup>-3</sup>) observed in this study, i.e., spring 2011, was around 40 % lower than that (397 ng m<sup>-3</sup>) in spring 2009. This result is ascribed to the fact that Chengdu municipal government established a special management committee to control biomass burning in suburban areas.

The fourth source factor is the iron and steel industry, characterized by high Fe, Mn, Zn, Pb, Cu, Cr, As, and Ga concentrations (Fig. 6d). This factor contributed 11 ± 9 % to the PM<sub>2.5</sub> mass concentration (Table 4). From single-particle analyses, enrichment of Fe, Zn, and Pb was observed in ambient atmospheric particles around a major integrated steelwork in the UK (Dall'Osto et al., 2008). China ranks as the largest iron and steel producer worldwide, whose productions constituted 44.2 % of the global production in 2010 (<http://www.miit.gov.cn/n11293472/n11293832/n11293907/n11368223/14344076.html>). However, only a few source apportionment studies identified this source in terms of its contributions to PM<sub>2.5</sub> pollution and PM-bound chemicals in China (Querol et al., 2006; Ni et al., 2012), despite that it was well recognized as a main source of pollutants, such as polycyclic aromatic hydrocarbons (PAHs) (Yang et al., 2002) and heavy metals (Machemer, 2004). Fe, Mn, and Cr in ambient aerosols collected around industrial sites were categorized into steel-related metals (Sweet et al., 1993). In the present study, we found a considerably practicable tracer – Ex-Fe – for this important emission source that seems to have been overlooked in China thus far. As illustrated in Fig. 8a, scatter plots of Fe versus Al in PM<sub>2.5</sub> of Chengdu show that most samples had Fe/Al mass ratios higher than 0.60, a characteristic ratio of Asian dust (Hsu et al., 2013, and references therein). During our sampling period, a dust storm sample was collected on April 30 2011 which gave rise to an Al maximum (3408 ng m<sup>-3</sup>). This sample had a Fe/Al ratio of 0.63 (Fig. 8a), in agreement with the typical ratio. The correlation result is also consistent with the EF<sub>crust</sub> result showing that the annual mean EF<sub>crust</sub> of Fe is 3.6 (Fig. 3), which is significantly higher than unity. This finding demonstrates that fine Fe aerosols originated from other nonnatural (i.e., anthropogenic) sources aside from dust. Likewise, the Mn/Al ratios ranged from 0.073

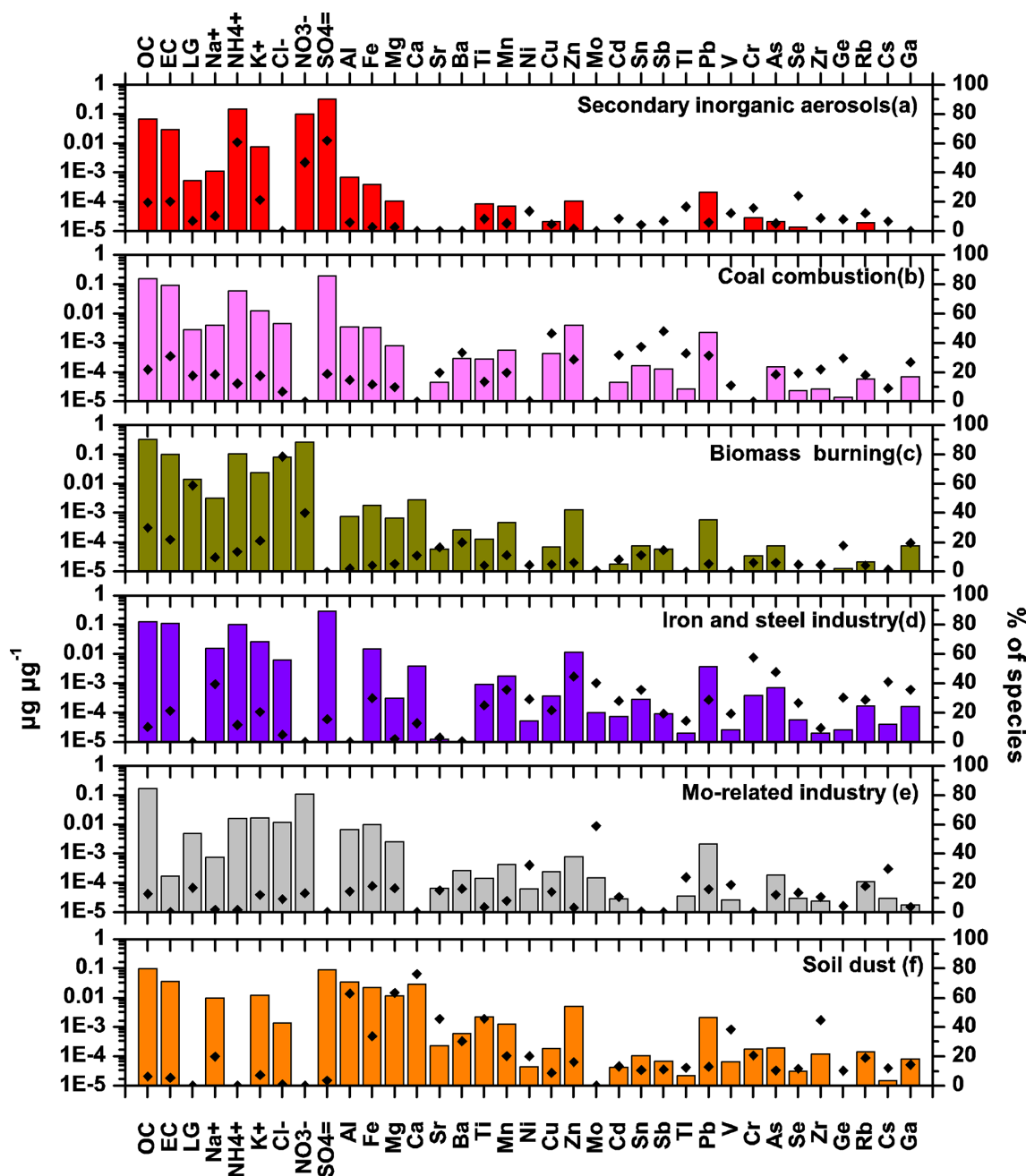


**Figure 6.** Six source profiles (bars) resolved from the PMF model (in units of  $\mu\text{g } \mu\text{g}^{-1}$ ). Also shown are contribution percentages (black dots) from each source factor.

to 0.145 in the four seasons (Fig. 8b), which is significantly larger than that (0.015) in average crust (Taylor, 1964). This result is indicative of enrichment and thus the dominance of other sources aside from natural dust. Accordingly, we defined Ex-Fe and excessive Mn (Ex-Mn) as follows:

$$[\text{Ex} - \text{Fe}] = [\text{Fe}_{\text{Measured}}] - [\text{Al}_{\text{Measured}}] \times 0.60,$$

$$[\text{Ex} - \text{Mn}] = [\text{Mn}_{\text{Measured}}] - [\text{Al}_{\text{Measured}}] \times 0.015.$$

where  $\text{Al}_{\text{Measured}}$ ,  $\text{Fe}_{\text{Measured}}$ , and  $\text{Mn}_{\text{Measured}}$  denote the measured concentrations of Al, Fe, and Mn, respectively, and the factors of 0.60 and 0.015 are the Fe/Al and Mn/Al mass ratios, respectively, in average crust composition. We then compared the derived time series of Ex-Fe and the iron and steel source contribution and found that they have a strong correlation ( $R^2 = 0.72$ ). Furthermore, we explored the correlations of steel-related metals, such as Mn, Ex-Mn, Zn, and Cr, against the derived Ex-Fe (Machemer, 2004), as depicted

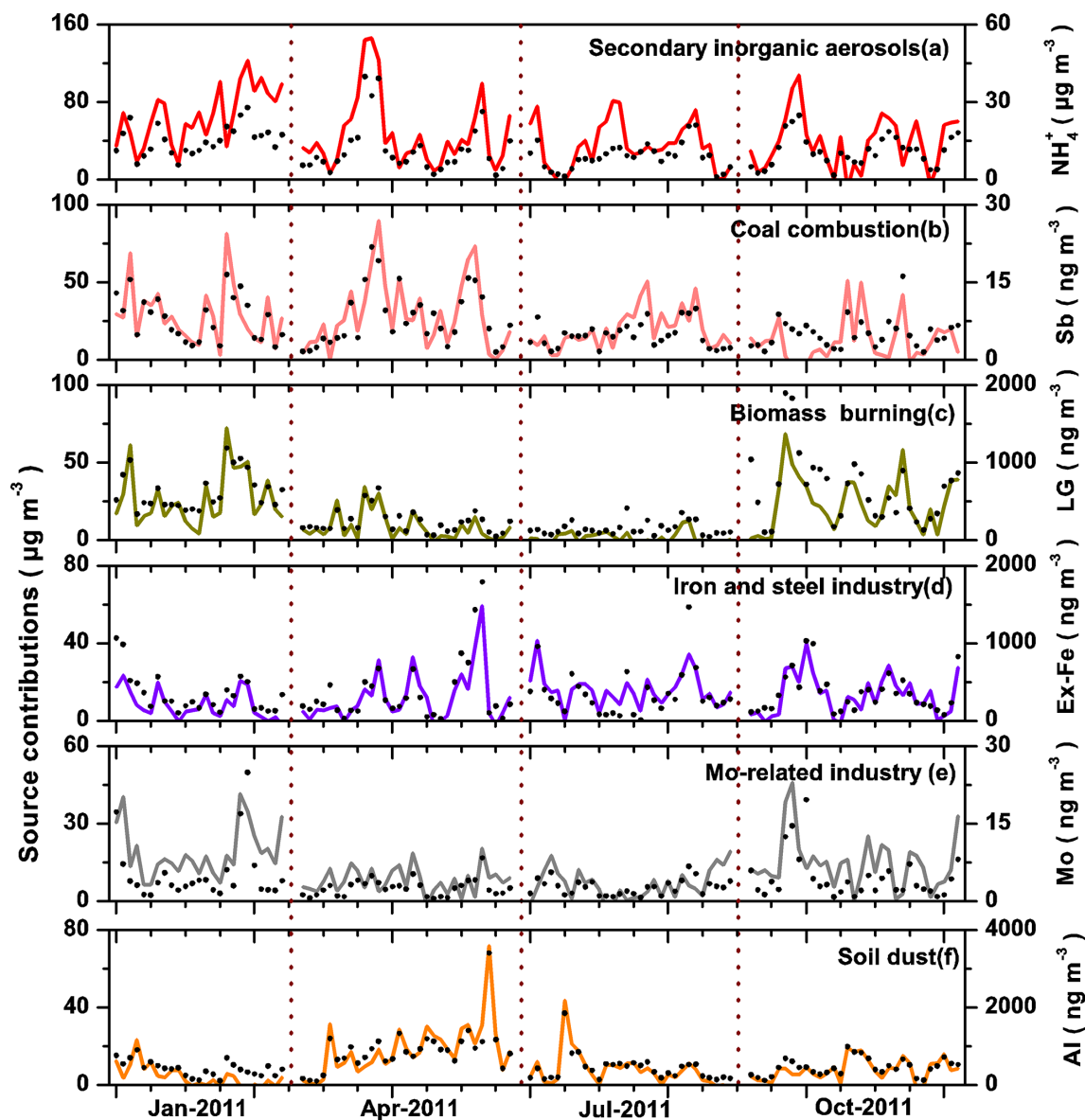


**Figure 7.** Time series of daily contributions from each identified source (continuous line) and specific chemical species (black dots) between January and October 2011.

in Supplement Fig. S4. Obvious linear correlations were observed, with an  $R^2$  ranging from 0.28 to 0.81, demonstrating that the iron and steel industry could be a vital source, in agreement with the PMF results (Fig. 6d).

Notably, the iron and steel manufacturing sources contributed more As than coal combustion sources in Chengdu (i.e., 48 versus 19%) (Fig. 6d). Along with Se (Hsu et al., 2009), arsenic is considered one of the more useful tracers of coal combustion. The As/Se ratio in PM<sub>2.5</sub> in Chengdu averaged  $6.8 \pm 2.6$ , which is much higher than that in coal combustion emission in Sichuan (1.1) and across China (0.94) (Tian et al., 2010). This finding suggests that coal combustion is not the main contributor of fine aerosol

As and merits further investigation in other provinces/cities, which would facilitate emission estimation of this carcinogenic metal across China. Moreover, contributions from this source to PM<sub>2.5</sub> varied significantly with season, ranging from  $19 \pm 9\%$  in summer to  $11 \pm 8\%$  in autumn,  $8 \pm 7\%$  in spring, and  $5 \pm 4\%$  in winter. Seasonality may be relevant to variability in production capacities of iron smelting factories. In fact, air pollutants (SO<sub>2</sub>, NO<sub>2</sub>, and PM<sub>10</sub>) emitted from certain most productive manufacturers around Chengdu were higher in summer than in other seasons based on routine monitoring results.

The fifth source is the Mo-related industries, characterized by high Mo and Ni. This source contributed  $11 \pm 9\%$

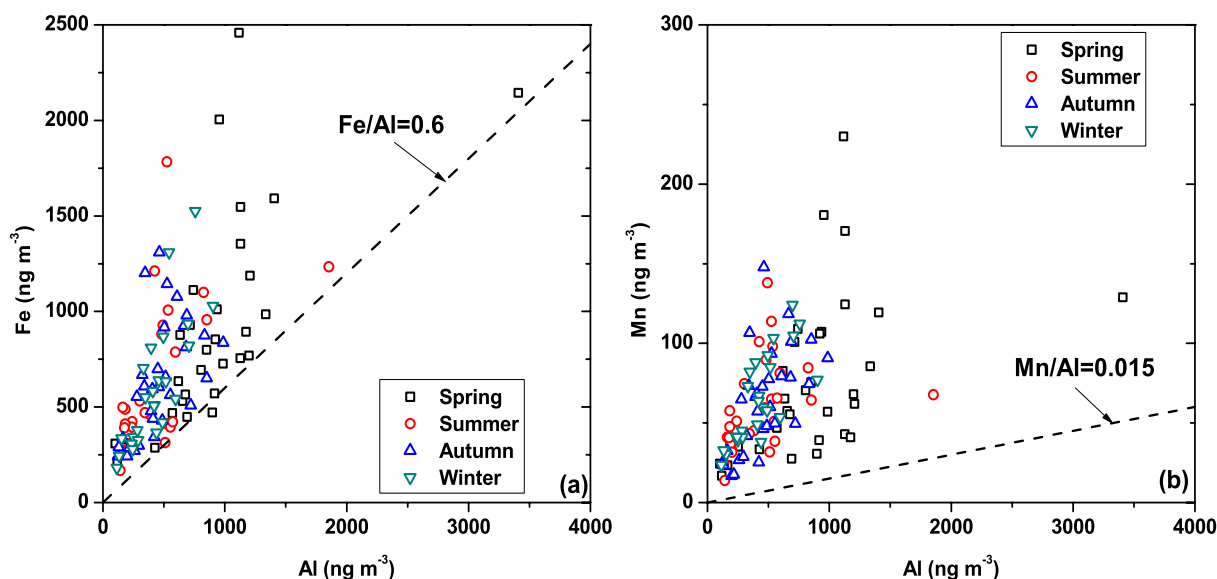


Figure 8. Scatter plots of Fe versus Al and Mn versus Al in PM<sub>2.5</sub> of Chengdu.

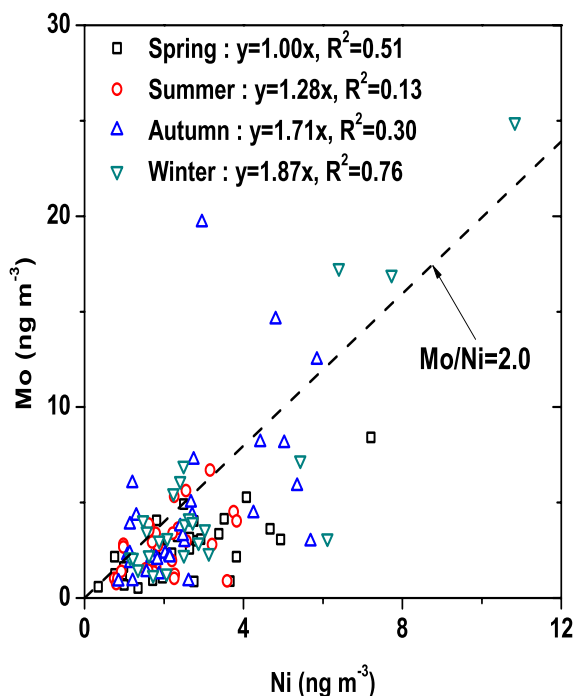


Figure 9. Scatter plots of Mo and Ni in four seasons.

to the PM<sub>2.5</sub> mass concentration but varied seasonally, e.g.,  $14 \pm 7\%$  in autumn,  $13 \pm 5\%$  in winter,  $11 \pm 14\%$  in summer, and  $8 \pm 5\%$  in spring (Table 4). Six samples had Mo concentrations over  $10 \text{ ng m}^{-3}$ ; of these three occurred in autumn and the other three in winter. The  $EF_{\text{crust}}$  values of Mo and Ni in fine aerosols in Chengdu were  $\sim 500$  and  $\sim 30$  (Fig. 3), respectively, which are much higher than unity,

indicative of the dominance of anthropogenic origins. Atmospheric Mo can originate from traffic emission, biomass burning, and industrial activities (Tsukuda et al., 2005; Dongarrà et al., 2007; Alleman et al., 2010). It usually has a concentration lower than  $1 \text{ ng m}^{-3}$  (Negral et al., 2008; Alleman et al., 2010; Mooiborek et al., 2011); in contrast, measurements in this study showed a mean concentration of  $3.8 \pm 3.8 \text{ ng m}^{-3}$ . Sn, Sb, and Cr were not found in the source profiles of this factor (Fig. 6e), suggesting that traffic emissions should not be a significant source for these elements, although Sb is often enriched in aerosols from vehicle emissions (Gómez et al., 2005; Varrica et al., 2013). A much higher OC/EC ratio ( $\sim 100$ ) also rules out the likelihood of traffic emission. This factor can be discriminated from the second and fourth factors, i.e., coal combustion and the iron and steel industry, as the missing three metals are representatives of the latter two source factors, as discussed above. For Ni, heavy oil combustion has often been suggested to be its most important anthropogenic source along with non-ferrous smelters (Sweet et al., 1993). Heavy oil combustion in Chengdu appeared to be an insignificant source for Ni, as the V/Ni ratio was averaged only  $0.7 \pm 0.3$ , which is much lower than the value (2–4) characterized for this industry sector (Almeida et al., 2005; Mamane et al., 2008). Furthermore, Mo and Ni correlated with each other in every season (Fig. 9), despite that their ratio (Mo/Ni) varied with season with higher ratios (1.7–1.9) in autumn and winter and lower ratios (1.0–1.3) in spring and summer. This trait is a distinctive feature (Mo-rich and Ni-deplete) from what is usually found in ambient atmosphere, e.g., a ratio significantly lower than unity (Negral et al., 2008; Mooibroek et al., 2011; Alleman et al., 2010). This factor may indicate the existence of a specific Mo source with a characteristic Mo/Ni ratio of

**Table 5.** Summary of measures taken by local and national government in Chengdu.

Source	Measures taken by local government	Measures taken by national government
Secondary inorganic aerosols	All industrial factories relocated out Chengdu urban area	Industrial emission standard
Coal combustion	Coal combustion forbidden in urban area	Industrial emission standard
Biomass burning	Special management committee established	None
Iron and steel industry	None	Industrial emission standard
Mo-related industries	None	None
Traffic emissions	Hybrid electric vehicles used in public transportation system	Emission standards for new vehicles
Soil dust	None	None

2.0 or higher, as demonstrated by the dashed line in Fig. 9. It is thus designated as Mo-related industries, which warrants further investigation, particularly in terms of which specific industry it belongs to. This finding is comparable with the result in Pittsburgh, where source apportionment studies have found Mo and Cr association with a source factor called the specialty steel factor (Pekney et al., 2006). The time series of this source contribution and the observed Mo concentrations correlated well, with an  $R^2$  of 0.47.

The sixth source factor is soil dust, which is characterized by elevated Al, Fe, Mg, Ca, Sr, Ti, V, and Zr. A few previous studies have found that Ca could have originated from anthropogenic activities in China and thus argued that Ca could serve as a marker for cement and construction dust (Zhang et al., 2005; Liu et al., 2005). However, the chemical profile of this identified source shows that Ca content is only 7.2% (Fig. 6f), which is much lower than that of cement ( $\sim 30\%$ ) and close to that in the northern China dust (7%) (Zhang et al., 2003). This indicates that cement and construction dust should not be a significant dust source in Chengdu. This factor accounted for  $10 \pm 10\%$  of the PM<sub>2.5</sub> mass concentration, which is lower than that in Beijing (15%) (Zhang et al., 2013). The contribution of soil dust to PM<sub>2.5</sub> mass concentrations was much higher in spring ( $18 \pm 17\%$ ) than in other seasons ( $9 \pm 12$ ,  $8 \pm 7$ , and  $4 \pm 5\%$  in summer, autumn, and winter, respectively). This seasonal pattern is also consistent with that of the FS concentration. The soil dust factor covers desert dust that usually prevails in spring and comes from north China via long-range transport, fugitive dust, and street dust, among which the latter two were dominated by local sources. Al, Fe, Ca, and Ti are typically major crustal elements that are often used to calculate soil dust mass concentration (Malm et al., 1994), similar to what was done in the current study. The EFs of Al, Fe, Mg, Ca, Sr, Ti, V, and Zr were lower than 10, indicative of the dominance of a natural mineral origin. Aluminum is a good tracer of soil dust. As expected, the time series of soil dust contribution and Al concentrations were consistent (Fig. 7f), with an  $R^2$  of 0.85.

### 3.4 Implications for PM alleviation

Efforts have been exerted to improve air quality in Chengdu in the past 5 years, as summarized in Table 5, most of which were based on the official information and/or documents available at the Chengdu governmental website (<http://www.chengdu.gov.cn/>). The Chengdu municipal government decreed that all industrial factories must be relocated out of the Chengdu urban area by the end of 2007. Commercial and residential coal combustion was banned in urban areas. A special management committee was established for controlling biomass burning in suburban areas. New light motor vehicles have been evaluated using the Chinese state emission standard IV since 2011. Heavy motor vehicles were banned in central urban areas and were evaluated using Chinese state emission standard III in 2013. Hybrid electric vehicles have been widely used in the public transportation system in recent years. These control strategies have not effectively alleviated the PM<sub>2.5</sub> pollution. The annual mean concentration of PM<sub>2.5</sub> in Chengdu was still nearly 3 times higher than NAAQS ( $35 \mu\text{g m}^{-3}$ ), implying that tremendous efforts are still needed.

Our study offers new insights into the causes of the elevated PM<sub>2.5</sub> levels. Despite the fact that all industrial enterprises in Chengdu urban areas had been relocated, most of these were resettled in Qingbaijiang industrial zone and Jintang county, which are situated in the upwind region around 20 km north of Chengdu. According to the spatial distribution of the fine AOD retrieved from Moderate Resolution Imaging Spectrometer sensors onboard Terra and Aqua satellites (Fig. 1), the highest AOD values ( $>0.6$ ) distributed in the Sichuan Basin are centered at the two biggest cities (Chengdu and Chongqing). Effective measures are also needed over the entire basin. Air mass back trajectories calculated using the NOAA HYSPLIT 4 trajectory model (Fig. 10) showed that air masses arrived at CRAES station at 500 and 1500 m levels but originated from the northeastern and western directions, often passing over the cities of Deyang, Mianyang, and Meishan, where many emission-producing industries are located. The combination of source apportionment results in conjunction with satellite AOD image and trajectory analyses suggest the dominance of local

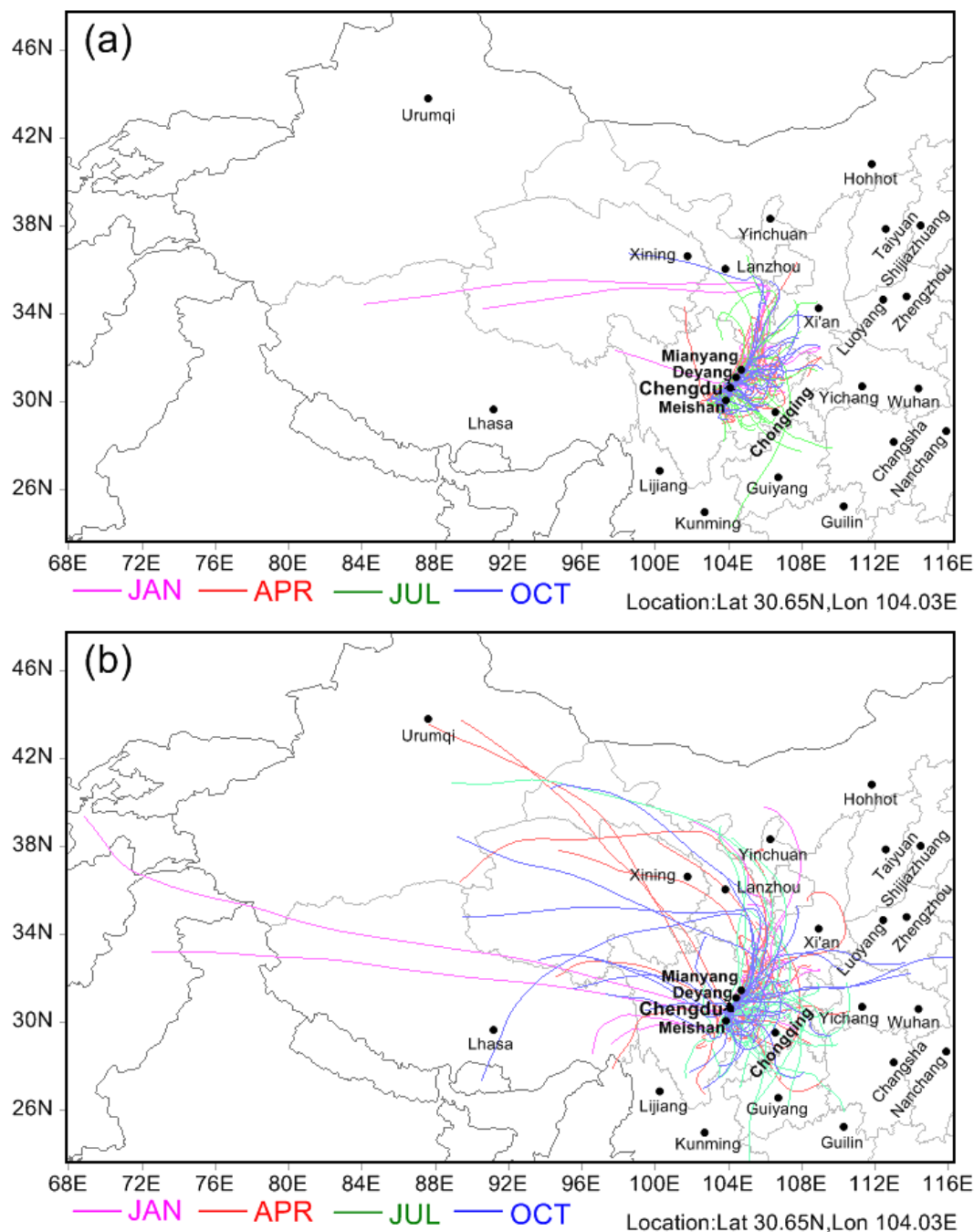


**Figure 10.** Analytical results of the 48 h air mass back trajectories at 500 m (a) and 1500 m (b) elevation during the sampling periods, which were run four times per day.

anthropogenic sources instead of regional and/or natural sources.

According to the PMF results, fossil-fuel-combustion-related activities including source factors of secondary inorganic aerosols, coal combustion, iron and steel manufacturing, and Mo-related industries contributed nearly 80 % to PM<sub>2.5</sub> and 96 % to sulfate aerosols. Therefore, coal quality in terms of sulfur and heavy metal content, and coal usage

in Sichuan province, should be managed, whereas PM concentration in coal-combustion-generated emissions should be abated. It is noted that traffic emission was not identified as a major factor by the PMF although the number of motor vehicles in Chengdu has exceeded 2 million. This raised the postulation that the management of traffic pollution might be effective to certain extent and that the traffic emission is relatively insignificant in contributing to the PM<sub>2.5</sub> pollution.

It should be noted that emissions from the traffic might be incorporated into the source factor of soil dust as its weighting contents of Zn, Pb, Cu, Sn, and Sb were relatively elevated, and might also be incorporated into the factor of secondary inorganic aerosols. Thus, more studies are needed to explore the contributions of traffic emissions to PM<sub>2.5</sub> pollution. In addition, biomass burning activities are presently a tough issue for China's environmental protection administration. Biomass fuel is widely used for cooking in rural areas in China. Waste straw produced in harvest seasons is habitually burned for fertilizing soils. The law forbidding straw burning was only enacted recently. A common strategy used by small boiler industries in Sichuan is to replace coal with biomass fuel as an energy source considering that sulfur dioxide emissions from biomass fuels may be much lower than from coal (Andreae and Merlet, 2001). However, more effort is needed in reducing air pollutant emissions from small boilers, which requires establishing new air pollutant emission standards for biomass fuel boilers. Rigorous efforts should be jointly exerted by different regions and cities and at various levels of the government.

#### 4 Conclusions

The annual average PM<sub>2.5</sub> concentration reached  $119 \pm 56 \mu\text{g m}^{-3}$  in 2011 in Chengdu, an inland megacity of southwest China. A typical seasonality of waxing in winter and waning in summer was observed. The annual PM<sub>2.5</sub> level in this city was three times greater than the NAAQS standard ( $35 \mu\text{g m}^{-3}$ ) and higher than those in many cities around the world. The annual mean concentration of carcinogenic As in Chengdu was up to  $20 \pm 11 \text{ ng m}^{-3}$ , which is also 3 times higher than the WHO's guide value ( $6.6 \text{ ng m}^{-3}$ ). Based on the results of chemical measurements and ISORROPIA-II thermodynamic equilibrium model results, major components of fine aerosols were identified to be inorganic ions, organic matter, elemental carbon, mineral soils, trace element oxides, and water, the sum of which accounted for  $92 \pm 11 \%$  of the observed masses.

Six source factors were identified using the PMF source apportionment model. The absolute ( $\mu\text{g m}^{-3}$ ) and fractional (%) contributions from each source factor varied with season. Distinctive chemical species were successfully used as characteristic tracers of individually modeled sources to validate source apportionment results. Biomarkers of biomass burning, LG and MN, were applied to constrain the more likely biomass burning sources. Wood burning was identified to be the main source in winter, while agricultural waste burning was the main source in autumn. The present study found a straightforward surrogate of iron and steel manufacturing pollution, namely excessive Fe, which is well correlated to the contribution from this source. A special source, Mo-related heavy industries, was modeled by PMF, corresponding to a persistently high Mo/Ni ratio of  $\geq 1.0$

throughout the sampling period. A preliminary hypothesis could be that the special source was relevant to specific alloy industries and/or military industries, pending further investigations.

The high PM<sub>2.5</sub> levels in Chengdu were mainly dominated by local anthropogenic emissions in the territory of the Sichuan Basin, in contrast to those found in Beijing. The unique topography surrounding the city is conducive to air pollutant accumulation and enhanced PM<sub>2.5</sub> pollution. Stricter emission standards are needed to alleviate elevated PM<sub>2.5</sub> loadings in this region. The source apportionment results presented here could serve as a valuable scientific basis for enacting effective emission control measures and policies.

**The Supplement related to this article is available online at doi:10.5194/acp-14-8679-2014-supplement.**

*Acknowledgements.* This study was supported by the Special Scientific Research Funds for National Basic Research Program of China (2013FY112700) and the Environment Protection Commonwealth Section (201009001).

Edited by: X. Tie

#### References

- Alleman, L. Y., Lamaison, L., Perdrix, E., Robache, A., and Galloo, J.-C.: PM<sub>10</sub> metal concentrations and source identification using positive matrix factorization and wind sectoring in a French industrial zone, *Atmos. Res.*, 96, 612–625, doi:10.1016/j.atmosres.2010.02.008, 2010.
- Almeida, S., Pio, C., Freitas, M., Reis, M., and Trancoso, M.: Source apportionment of fine and coarse particulate matter in a sub-urban area at the Western European Coast, *Atmos. Environ.*, 39, 3127–3138, doi:10.1016/j.atmosenv.2005.01.048, 2005.
- Andreae, M. O. and Merlet, P.: Emission of trace gases and aerosols from biomass burning, *Global Biogeochem. Cy.*, 15, 955–966, doi:10.1029/2000GB001382, 2001.
- Andreae, M. O. and Rosenfeld, D.: Aerosol–cloud–precipitation interactions. Part 1. The nature and sources of cloud-active aerosols, *Earth-Sci. Rev.*, 89, 13–41, doi:10.1016/j.earscirev.2008.03.001, 2008.
- Balasubramanian, R., Qian, W., Decesari, B. S., Facchini, M. C., and Fuzzi, S. Comprehensive characterization of PM<sub>2.5</sub> aerosols in Singapore, *J. Geophys. Res.*, 108, 4523, doi:10.1029/2002JD002517, 2003.
- Cao, G., Zhang, X., and Zheng, F.: Inventory of black carbon and organic carbon emissions from China, *Atmos. Environ.*, 40, 6516–6527, doi:10.1016/j.atmosenv.2006.05.070, 2006.
- Cao, J., Lee, S., Ho, K., Zhang, X., Zou, S., Fung, K., Chow, J. C., and Watson, J. G.: Characteristics of carbonaceous aerosol in Pearl River Delta Region, China during 2001 winter period, *Atmos. Environ.*, 37, 1451–1460, doi:10.1016/S1352-2310(02)01002-6, 2003.

- Cao, J., Lee, S., Chow, J. C., Watson, J. G., Ho, K., Zhang, R., Jin, Z., Shen, Z., Chen, G., and Kang, Y.: Spatial and seasonal distributions of carbonaceous aerosols over China, *J. Geophys. Res.-Atmos.*, 112, D22S11, doi:10.1029/2006JD008205, 2007.
- Chen, L.-W. A., Lowenthal, D. H., Watson, J. G., Koracin, D., Kumar, N., Knipping, E. M., Wheeler, N., Craig, K., and Reid, S.: Toward effective source apportionment using positive matrix factorization: experiments with simulated PM<sub>2.5</sub> data, *J. Air Waste Manage. Assoc.*, 60, 43–54, doi:10.3155/1047-3289.60.1.43, 2010.
- Chow, J. C., Watson, J. G., Chen, L.-W. A., Chang, M. O., Robinson, N. F., Trimble, D., and Kohl, S.: The IMPROVE\_A temperature protocol for thermal/optical carbon analysis: maintaining consistency with a long-term database, *J. Air Waste Manage. Assoc.*, 57, 1014–1023, doi:10.3155/1047-3289.57.9.1014, 2007.
- Dall'Osto, M., Booth, M., Smith, W., Fisher, R., and Harrison, R. M.: A study of the size distributions and the chemical characterization of airborne particles in the vicinity of a large integrated steelworks, *Aerosol Sci. Technol.*, 42, 981–991, doi:10.1080/02786820802339587, 2008.
- Dan, M., Zhuang, G., Li, X., Tao, H., and Zhuang, Y.: The characteristics of carbonaceous species and their sources in PM<sub>2.5</sub> in Beijing, *Atmos. Environ.*, 38, 3443–3452, doi:10.1016/j.atmosenv.2004.02.052, 2004.
- Dongarrà, G., Manno, E., Varrica, D., and Vultaggio, M.: Mass levels, crustal component and trace elements in PM<sub>10</sub> in Palermo, Italy, *Atmos. Environ.*, 41, 7977–7986, doi:10.1016/j.atmosenv.2007.09.015, 2007.
- Draxler, R. R. and Rolph, G. D.: HYSPLIT (HYbrid Single-Particle Lagrangian Integrated Trajectory) Model Access via NOAA ARL READY Website, available at: <http://www.arl.noaa.gov/HYSPLIT.php>, NOAA Air Resources Laboratory, College Park, MD.
- Duan, F., Liu, X., Yu, T., and Cachier, H.: Identification and estimate of biomass burning contribution to the urban aerosol organic carbon concentrations in Beijing, *Atmos. Environ.*, 38, 1275–1282, doi:10.1016/j.atmosenv.2003.11.037, 2004.
- Eder, B. and Yu, S.: A performance evaluation of the 2004 release of Models-3 CMAQ, *Atmos. Environ.*, 40, 4811–4824, doi:10.1016/j.atmosenv.2005.08.045, 2006.
- Edwards, R. D., Smith, K. R., Zhang, J., and Ma, Y.: Implications of changes in household stoves and fuel use in China, *Energ. Policy*, 32, 395–411, doi:10.1016/S0301-4215(02)00309-9, 2004.
- Engling, G., Carrico, C. M., Kreidenweis, S. M., Collett Jr., J. L., Day, D. E., Malm, W. C., Lincoln, E., Min Hao, W., Iinuma, Y., and Herrmann, H.: Determination of levoglucosan in biomass combustion aerosol by high-performance anion-exchange chromatography with pulsed amperometric detection, *Atmos. Environ.*, 40, 299–311, doi:10.1016/j.atmosenv.2005.12.069, 2006.
- Engling, G., Lee, J. J., Tsai, Y.-W., Lung, S.-C. C., Chou, C. C.-K., and Chan, C.-Y.: Size-resolved anhydrosugar composition in smoke aerosol from controlled field burning of rice straw, *Aerosol Sci. Technol.*, 43, 662–672, doi:10.1080/02786820902825113, 2009.
- Feng, Y., Chen, Y., Guo, H., Zhi, G., Xiong, S., Li, J., Sheng, G., and Fu, J.: Characteristics of organic and elemental carbon in PM<sub>2.5</sub> samples in Shanghai, China, *Atmos. Res.*, 92, 434–442, doi:10.1016/j.atmosres.2009.01.003, 2009.
- Fountoukis, C. and Nenes, A.: ISORROPIA II: a computationally efficient thermodynamic equilibrium model for K<sup>+</sup> – Ca<sup>2+</sup> – Mg<sup>2+</sup> – H<sub>4</sub><sup>+</sup> – Na<sup>+</sup> – SO<sub>4</sub><sup>2-</sup> – NO<sub>3</sub><sup>-</sup> – Cl<sup>-</sup> – H<sub>2</sub>O aerosols, *Atmos. Chem. Phys.*, 7, 4639–4659, doi:10.5194/acp-7-4639-2007, 2007.
- Gómez, D. R., Giné, M. F., Bellato, A. C. S., and Smichowski, P.: Antimony: a traffic-related element in the atmosphere of Buenos Aires, Argentina, *J. Environ. Monit.*, 7, 1162–1168, doi:10.1039/B508609D, 2005.
- Gregg, J. S., Andres, R. J., and Marland, G.: China: Emissions pattern of the world leader in CO<sub>2</sub> emissions from fossil fuel consumption and cement production, *Geophys. Res. Lett.*, 35, L08806, doi:10.1029/2007GL032887, 2008.
- Gu, J., Bai, Z., Liu, A., Wu, L., Xie, Y., Li, W., Dong, H., and Zhang, X.: Characterization of Atmospheric Organic Carbon and Elemental Carbon of PM<sub>2.5</sub> and PM<sub>10</sub> at Tianjin, China, *Aerosol Air Qual. Res.*, 10, 167–176, doi:10.4209/aaqr.2009.12.0080, 2010.
- Hans Wedepohl, K.: The composition of the continental crust, *Geochim. Cosmochim. Acta*, 59, 1217–1232, doi:10.1016/0016-7037(95)00038-2, 1995.
- He, K., Yang, F., Ma, Y., Zhang, Q., Yao, X., Chan, C. K., Cadle, S., Chan, T., and Mulawa, P.: The characteristics of PM<sub>2.5</sub> in Beijing, China, *Atmos. Environ.*, 35, 4959–4970, doi:10.1016/S1352-2310(01)00301-6, 2001.
- Heo, J. B., Hopke, P. K., and Yi, S. M.: Source apportionment of PM<sub>2.5</sub> in Seoul, Korea, *Atmos. Chem. Phys.*, 9, 4957–4971, doi:10.5194/acp-9-4957-2009, 2009.
- Hsu, S.-C., Liu, S. C., Kao, S.-J., Jeng, W.-L., Huang, Y.-T., Tseng, C.-M., Tsai, F., Tu, J.-Y., and Yang, Y.: Water-soluble species in the marine aerosol from the northern South China Sea: High chloride depletion related to air pollution, *J. Geophys. Res.*, 112, D19304, doi:10.1029/2007JD008844, 2007.
- Hsu, S.-C., Liu, S. C., Huang, Y.-T., Lung, S.-C. C., Tsai, F., Tu, J.-Y., and Kao, S.-J.: A criterion for identifying Asian dust events based on Al concentration data collected from northern Taiwan between 2002 and early 2007, *J. Geophys. Res.*, 113, D18306, doi:10.1029/2007JD009574, 2008.
- Hsu, S. C., Liu, S. C., Huang, Y. T., Chou, C. C. K., Lung, S. C. C., Liu, T. H., Tu, J. Y., and Tsai, F.: Long-range southeastward transport of Asian biomass pollution: signature detected by aerosol potassium in Northern Taiwan, *J. Geophys. Res.*, 114, D14301, doi:10.1029/2009JD011725, 2009.
- Hsu, S., Liu, S., Tsai, F., Engling, G., Lin, I., Chou, C., Kao, S., Lung, S., Chan, C., and Lin, S.: High wintertime particulate matter pollution over an offshore island (Kinmen) off southeastern China: An overview, *J. Geophys. Res.-Atmos.*, 115, D17309, doi:10.1029/2009JD013641, 2010.
- Hsu, S. C., Tsai, F., Lin, F. J., Chen, W. N., Shiah, F. K., Huang Jr, C., Chan, C. Y., Chen, C. C., Liu, T. H., and Chen, H. Y.: A super Asian dust storm over the East and South China Seas: Disproportionate dust deposition, *J. Geophys. Res.-Atmos.*, 118, 7169–7181, doi:10.1002/jgrd.50405, 2013.
- Hueglin, C., Gehrig, R., Baltensperger, U., Gysel, M., Monn, C., and Vonmont, H.: Chemical characterisation of PM<sub>2.5</sub>, PM<sub>10</sub> and coarse particles at urban, near-city and rural sites in Switzerland, *Atmos. Environ.*, 39, 637–651, doi:10.1016/j.atmosenv.2004.10.027, 2005.
- Iinuma, Y., Engling, G., Puxbaum, H., and Herrmann, H.: A highly resolved anion-exchange chromatographic method for determi-

- nation of saccharidic tracers for biomass combustion and primary bio-particles in atmospheric aerosol, *Atmos. Environ.*, 43, 1367–1371, doi:10.1016/j.atmosenv.2008.11.020, 2009.
- Khan, M. F., Shirasuna, Y., Hirano, K., and Masunaga, S.: Characterization of PM<sub>2.5</sub>, PM<sub>2.5–10</sub> and PM<sub>10</sub> in ambient air, Yokohama, Japan, *Atmos. Res.*, 96, 159–172, doi:10.1016/j.atmosres.2009.12.009, 2010.
- Laden, F., Neas, L. M., Dockery, D. W., and Schwartz, J.: Association of fine particulate matter from different sources with daily mortality in six US cities, *Environ. Health Perspect.*, 108, 941–947, 2000.
- Lee, H. S. and Kang, B.-W.: Chemical characteristics of principal PM<sub>2.5</sub> species in Chongju, South Korea, *Atmos. Environ.*, 35, 739–746, doi:10.1016/S1352-2310(00)00267-3, 2001.
- Lei, Y., Zhang, Q., He, K., and Streets, D.: Primary anthropogenic aerosol emission trends for China, 1990–2005, *Atmos. Chem. Phys.*, 11, 931–954, doi:10.5194/acp-11-931-2011, 2011.
- Liu, X., Zhu, J., Van Espen, P., Adams, F., Xiao, R., Dong, S., and Li, Y.: Single particle characterization of spring and summer aerosols in Beijing: Formation of composite sulfate of calcium and potassium, *Atmos. Environ.*, 39, 6909–6918, doi:10.1016/j.atmosenv.2005.08.007, 2005.
- Lonati, G., Giugliano, M., Butelli, P., Romele, L., and Tardivo, R.: Major chemical components of PM<sub>2.5</sub> in Milan (Italy), *Atmos. Environ.*, 39, 1925–1934, doi:10.1016/j.atmosenv.2004.12.012, 2005.
- Louie, P. K., Watson, J. G., Chow, J. C., Chen, A., Sin, D. W., and Lau, A. K.: Seasonal characteristics and regional transport of PM<sub>2.5</sub> in Hong Kong, *Atmos. Environ.*, 39, 1695–1710, doi:10.1016/j.atmosenv.2004.11.017, 2005.
- Ma, Y., Chen, R., Pan, G., Xu, X., Song, W., Chen, B., and Kan, H.: Fine particulate air pollution and daily mortality in Shenyang, China, *Sci. Total Environ.* 409, 2473–2477, doi:10.1016/j.scitotenv.2011.03.017, 2011.
- Machemer, S. D.: Characterization of airborne and bulk particulate from iron and steel manufacturing facilities, *Environ. Sci. Technol.*, 38, 381–389, doi:10.1021/es020897v, 2004.
- Malm, W. C., Sisler, J. F., Huffman, D., Eldred, R. A., and Cahill, T. A.: Spatial and seasonal trends in particle concentration and optical extinction in the United States, *J. Geophys. Res.*, 99, 1347–1370, doi:10.1029/93JD02916, 1994.
- Mamane, Y., Perrino, C., Yossef, O., and Catrambone, M.: Source characterization of fine and coarse particles at the East Mediterranean coast, *Atmos. Environ.* 42, 6114–6130, doi:10.1016/j.atmosenv.2008.02.045, 2008.
- Mooibroek, D., Schaap, M., Weijers, E., and Hoogerbrugge, R.: Source apportionment and spatial variability of PM<sub>2.5</sub> using measurements at five sites in the Netherlands, *Atmos. Environ.*, 45, 4180–4191, doi:10.1016/j.atmosenv.2011.05.017, 2011.
- Mukai, H., Tanaka, A., Fujii, T., Zeng, Y., Hong, Y., Tang, J., Guo, S., Xue, H., Sun, Z., and Zhou, J.: Regional characteristics of sulfur and lead isotope ratios in the atmosphere at several Chinese urban sites, *Environ. Sci. Technol.*, 35, 1064–1071, doi:10.1021/es001399u, 2001.
- Negral, L., Moreno-Grau, S., Moreno, J., Querol, X., Viana, M., and Alastuey, A.: Natural and anthropogenic contributions to PM<sub>10</sub> and PM<sub>2.5</sub> in an urban area in the western Mediterranean coast, *Water Air Soil Pollut.*, 192, 227–238, doi:10.1007/s11270-008-9650-y, 2008.
- Ni, Z.-Y., Chen, Y.-J., Li, N., and Zhang, H.: Pb–Sr–Nd isotope constraints on the fluid source of the Dahu Au–Mo deposit in Qinling Orogen, central China, and implication for Triassic tectonic setting, *Ore Geol. Rev.*, 46, 60–67, doi:10.1016/j.oregeorev.2012.01.004, 2012.
- Norris, G., Vedantham, R., Wade, K., Brown, S., Prouty, J., and Foley, C.: EPA positive matrix factorization (PMF) 3.0 fundamentals & user guide, US Environmental Protection Agency, Office of Research and Development, Washington, DC, 2008.
- Oliveira, C., Pio, C., Alves, C., Evtyugina, M., Santos, P., Gonçalves, V., Nunes, T., Silvestre, A. J., Palmgren, F., and Wählin, P.: Seasonal distribution of polar organic compounds in the urban atmosphere of two large cities from the North and South of Europe, *Atmos. Environ.*, 41, 5555–5570, doi:10.1016/j.atmosenv.2007.03.001, 2007.
- Pacyna, J. M. and Pacyna, E. G.: An assessment of global and regional emissions of trace metals to the atmosphere from anthropogenic sources worldwide, *Environ. Rev.*, 9, 269–298, doi:10.1139/a01-012, 2001.
- Pekney, N. J., Davidson, C. I., Robinson, A., Zhou, L., Hopke, P., Eatough, D., and Rogge, W. F.: Major source categories for PM<sub>2.5</sub> in Pittsburgh using PMF and UNMIX, *Aerosol Sci. Technol.*, 40, 910–924, doi:10.1080/02786820500380271, 2006.
- Pinto, J. P., Lefohn, A. S., and Shadwick, D. S.: Spatial Variability of PM<sub>2.5</sub> in Urban Areas in the United States, *J. Air Waste Manage. Assoc.*, 54, 440–449, doi:10.1080/10473289.2004.10470919, 2004.
- Pio, C., Legrand, M., Alves, C., Oliveira, T., Afonso, J., Caseiro, A., Puxbaum, H., Sánchez-Ochoa, A., and Gelencsér, A.: Chemical composition of atmospheric aerosols during the 2003 summer intense forest fire period, *Atmos. Environ.*, 42, 7530–7543, doi:10.1016/j.atmosenv.2008.05.032, 2008.
- Pope III, C. A., and Dockery, D. W.: Health effects of fine particulate air pollution: lines that connect, *J. Air Waste Manage. Assoc.*, 56, 709–742, doi:10.1080/10473289.2006.10464485, 2006.
- Putaud, J.-P., Raes, F., Van Dingenen, R., Brüggemann, E., Facchini, M., Decesari, S., Fuzzi, S., Gehrig, R., Hüglin, C., and Laj, P.: A European aerosol phenomenology – 2: chemical characteristics of particulate matter at kerbside, urban, rural and background sites in Europe, *Atmos. Environ.*, 38, 2579–2595, doi:10.1016/j.atmosenv.2004.01.041, 2004.
- Qin, Y. and Xie, S.: Spatial and temporal variation of anthropogenic black carbon emissions in China for the period 1980–2009, *Atmos. Chem. Phys.*, 12, 4825–4841, doi:10.5194/acp-12-4825-2012, 2012.
- Querol, X., Alastuey, A., Ruiz, C., Artinano, B., Hansson, H., Harrison, R., Buringh, E. t., Ten Brink, H., Lutz, M., and Bruckmann, P.: Speciation and origin of PM<sub>10</sub> and PM<sub>2.5</sub> in selected European cities, *Atmos. Environ.*, 38, 6547–6555, doi:10.1016/j.atmosenv.2004.08.037, 2004.
- Querol, X., Zhuang, X., Alastuey, A., Viana, M., Lv, W., Wang, Y., López, A., Zhu, Z., Wei, H., and Xu, S.: Speciation and sources of atmospheric aerosols in a highly industrialised emerging mega-city in Central China, *J. Environ. Monit.*, 8, 1049–1059, doi:10.1039/B608768J, 2006.
- Remer, L. A., Kaufman, Y. J., Tanré, D., Mattoo, S., Chu, D. A., Martins, J. V., Li, R.-R., Ichoku, C., Levy, R. C., Kleidman, R. G., Eck, T. F., Vermote, E., and Holben, B. N.: The MODIS

- Aerosol Algorithm, Products, and Validation, *J. Atmos. Sci.*, 62, 947–973, doi:10.1175/JAS3385.1, 2005.
- Rolph, G. D.: Real-time Environmental Applications and Display system (READY) Website, available at: <http://www.ready.noaa.gov>, NOAA Air Resources Laboratory, College Park, MD, 2013.
- Seinfeld, J. H., Carmichael, G. R., Arimoto, R., Conant, W. C., Brechtel, F. J., Bates, T. S., Cahill, T. A., Clarke, A. D., Doherty, S. J., and Flatau, P. J.: ACE-ASIA-Regional climatic and atmospheric chemical effects of Asian dust and pollution, *B. Am. Meteorol. Soc.*, 85, 367–380, doi:10.1175/BAMS-85-3-367, 2004.
- Sheesley, R. J., Schauer, J. J., Chowdhury, Z., Cass, G. R., and Simoneit, B. R.: Characterization of organic aerosols emitted from the combustion of biomass indigenous to South Asia, *J. Geophys. Res.*, 108, 4285, doi:10.1029/2002JD002981, 2003.
- Simon, H., Bhave, P., Swall, J., Frank, N., and Malm, W.: Determining the spatial and seasonal variability in OM/OC ratios across the US using multiple regression, *Atmos. Chem. Phys.*, 11, 2933–2949, doi:10.5194/acp-11-2933-2011, 2011.
- Sternbeck, J., Sjödin, Å., and Andréasson, K.: Metal emissions from road traffic and the influence of resuspension – results from two tunnel studies, *Atmos. Environ.* 36, 4735–4744, doi:10.1016/S1352-2310(02)00561-7, 2002.
- Sweet, C. W., Vermette, S. J., and Landsberger, S.: Sources of toxic trace elements in urban air in Illinois, *Environ. Sci. Technol.*, 27, 2502–2510, doi:10.1021/es00048a030, 1993.
- Szidat, S., Jenk, T. M., Synal, H. A., Kalberer, M., Wacker, L., Hajas, I., Kasper-Giebl, A., and Baltensperger, U.: Contributions of fossil fuel, biomass burning, and biogenic emissions to carbonaceous aerosols in Zurich as traced by <sup>14</sup>C, *J. Geophys. Res.-Atmos.*, 111, D07206, doi:10.1029/2005JD006590, 2006.
- Szidat, S., Ruff, M., Perron, N., Wacker, L., Synal, H.-A., Hallquist, M., Shannigrahi, A. S., Yttri, K., Dye, C., and Simpson, D.: Fossil and non-fossil sources of organic carbon (OC) and elemental carbon (EC) in Göteborg, Sweden, *Atmos. Chem. Phys.*, 9, 1521–1535, doi:10.5194/acp-9-1521-2009, 2009.
- Tao, J., Shen, Z., Zhu, C., Yue, J., Cao, J., Liu, S., Zhu, L., and Zhang, R.: Seasonal variations and chemical characteristics of sub-micrometer particles (PM<sub>1</sub>) in Guangzhou, China, *Atmos. Res.*, 115, 222–231, doi:10.1016/j.atmosres.2012.06.025, 2012.
- Tao, J., Zhang, L., Engling, G., Zhang, R., Yang, Y., Cao, J., Zhu, C., Wang, Q., and Luo, L.: Chemical composition of PM<sub>2.5</sub> in an urban environment in Chengdu, China: Importance of springtime dust storms and biomass burning, *Atmos. Res.*, 122, 270–283, doi:10.1016/j.atmosres.2012.11.004, 2013.
- Tao, J., Zhang, L., Ho, K., Zhang, R., Lin, Z., Zhang, Z., Lin, M., Cao, J., Liu, S., and Wang, G.: Impact of PM<sub>2.5</sub> chemical compositions on aerosol light scattering in Guangzhou – the largest megacity in South China, *Atmos. Res.*, 135–136, 48–58, doi:10.1016/j.atmosres.2013.08.015, 2014.
- Taylor, S. R.: Trace element abundances and the chondritic Earth model, *Geochim. Cosmochim. Ac.*, 28, 1989–1998, doi:10.1016/0016-7037(64)90142-5, 1964.
- Tian, H., Wang, Y., Xue, Z., Cheng, K., Qu, Y., Chai, F., and Hao, J.: Trend and characteristics of atmospheric emissions of Hg, As, and Se from coal combustion in China, 1980–2007, *Atmos. Chem. Phys.*, 10, 11905–11919, doi:10.5194/acp-10-11905-2010, 2010.
- Tian, H., Zhao, D., Cheng, K., Lu, L., He, M., and Hao, J.: Anthropogenic atmospheric emissions of antimony and its spatial distribution characteristics in China, *Environ. Sci. Technol.*, 46, 3973–3980, doi:10.1021/es2041465, 2012.
- Tsukuda, S., Sugiyama, M., Harita, Y., and Nishimura, K.: Atmospheric bulk deposition of soluble phosphorus in Ashiu Experimental Forest, Central Japan: source apportionment and sample contamination problem, *Atmos. Environ.* 39, 823–836, doi:10.1016/j.atmosenv.2004.10.028, 2005.
- Turpin, B. J. and Huntzicker, J. J.: Identification of secondary organic aerosol episodes and quantitation of primary and secondary organic aerosol concentrations during SCAQS, *Atmos. Environ.*, 29, 3527–3544, doi:10.1016/1352-2310(94)00276-Q, 1995.
- Turpin, B. J. and Lim, H.-J.: Species contributions to PM<sub>2.5</sub> mass concentrations: Revisiting common assumptions for estimating organic mass, *Aerosol Sci. Technol.*, 35, 602–610, doi:10.1080/02786820119445, 2001.
- Varrica, D., Bardelli, F., Dongarrà, G., and Tamburo, E.: Speciation of Sb in airborne particulate matter, vehicle brake linings, and brake pad wear residues, *Atmos. Environ.*, 64, 18–24, doi:10.1016/j.atmosenv.2012.08.067, 2013.
- Wang, X., Zhang, L., and Moran, M.: Uncertainty assessment of current size-resolved parameterizations for below-cloud particle scavenging by rain, *Atmos. Chem. Phys.*, 10, 5685–5705, doi:10.5194/acp-10-5685-2010, 2010.
- Watson, J. G.: Visibility: Science and regulation, *J. Air Waste Manage. Assoc.*, 52, 628–713, doi:10.1080/10473289.2002.10470813, 2002.
- Watson, J. G., Chow, J. C., and Houck, J. E.: PM<sub>2.5</sub> chemical source profiles for vehicle exhaust, vegetative burning, geological material, and coal burning in Northwestern Colorado during 1995, *Chemosphere*, 43, 1141–1151, doi:10.1016/S0045-6535(00)00171-5, 2001.
- World Health Organization: Regional Office for Europe, Air quality guidelines for Europe, No. 91, WHO Regional Office Europe, 2000.
- Xing, L., Fu, T.-M., Cao, J., Lee, S., Wang, G., Ho, K., Cheng, M.-C., You, C.-F., and Wang, T.: Seasonal and spatial variability of the OM/OC mass ratios and high regional correlation between oxalic acid and zinc in Chinese urban organic aerosols, *Atmos. Chem. Phys.*, 13, 4307–4318, doi:10.5194/acp-13-4307-2013, 2013.
- Xu, H., Cao, J., Ho, K., Ding, H., Han, Y., Wang, G., Chow, J., Watson, J., Khol, S., and Qiang, J.: Lead concentrations in fine particulate matter after the phasing out of leaded gasoline in Xi'an, China, *Atmos. Environ.*, 46, 217–224, doi:10.1016/j.atmosenv.2011.09.078, 2012a.
- Xu, L., Chen, X., Chen, J., Zhang, F., He, C., Zhao, J., and Yin, L.: Seasonal variations and chemical compositions of PM<sub>2.5</sub> aerosol in the urban area of Fuzhou, China, *Atmos. Res.*, 104, 264–272, doi:10.1016/j.atmosres.2011.10.017, 2012b.
- Yan, X., Ohara, T., and Akimoto H.: Bottom-up estimate of biomass burning in mainland China, *Atmos. Environ.*, 40, 5262–5273, doi:10.1016/j.atmosenv.2006.04.040, 2006.
- Yang, F., Tan, J., Zhao, Q., Du, Z., He, K., Ma, Y., Duan, F., and Chen, G.: Characteristics of PM<sub>2.5</sub> speciation in representative megacities and across China, *Atmos. Chem. Phys.*, 11, 5207–5219, doi:10.5194/acp-11-5207-2011, 2011.
- Yang, H.-H., Lai, S.-O., Hsieh, L.-T., Hsueh, H.-J., and Chi, T.-W.: Profiles of PAH emission from steel and iron industries, Chemo-

- sphere, 48, 1061–1074, doi:10.1016/S0045-6535(02)00175-3, 2002.
- Ye, B., Ji, X., Yang, H., Yao, X., Chan, C. K., Cadle, S. H., Chan, T., and Mulawa, P. A.: Concentration and chemical composition of PM<sub>2.5</sub> in Shanghai for a 1-year period, *Atmos. Environ.*, 37, 499–510, doi:10.1016/S1352-2310(02)00918-4, 2003.
- Yttri, K., Dye, C., Braathen, O.-A., Simpson, D., and Steinnes, E.: Carbonaceous aerosols in Norwegian urban areas, *Atmos. Chem. Phys.*, 8, 2007–2020, doi:10.5194/acp-9-2007-2009, 2009.
- Zdráhal, Z., Oliveira, J., Vermeylen, R., Claeys, M., and Maenhaut, W.: Improved method for quantifying levoglucosan and related monosaccharide anhydrides in atmospheric aerosols and application to samples from urban and tropical locations, *Environ. Sci. Technol.*, 36, 747–753, doi:10.1021/es015619v, 2002.
- Zhang, D., Shi, G., Iwasaka, Y., Hu, M., and Zang, J.: Anthropogenic calcium particles observed in Beijing and Qingdao, China, *Water Air Soil Pollut.*, 5, 261–276, doi:10.1007/s11267-005-0743-y, 2005.
- Zhang, F., Xu, L., Chen, J., Yu, Y., Niu, Z., and Yin, L.: Chemical compositions and extinction coefficients of PM<sub>2.5</sub> in peri-urban of Xiamen, China, during June 2009–May 2010, *Atmos. Res.*, 106, 150–158, doi:10.1016/j.atmosres.2011.12.005, 2012.
- Zhang, R., Jing, J., Tao, J., Hsu, S. C., Wang, G., Cao, J., Lee, C. S. L., Zhu, L., Chen, Z., Zhao, Y., and Shen, Z.: Chemical characterization and source apportionment of PM<sub>2.5</sub> in Beijing: seasonal perspective, *Atmos. Chem. Phys.*, 13, 7053–7074, doi:10.5194/acp-13-7053-2013, 2013.
- Zhang, T., Cao, J., Tie, X., Shen, Z., Liu, S., Ding, H., Han, Y., Wang, G., Ho, K., and Qiang, J.: Water-soluble ions in atmospheric aerosols measured in Xi'an, China: seasonal variations and sources, *Atmos. Res.*, 102, 110–119, doi:10.1016/j.atmosres.2011.06.014, 2011.
- Zhang, X. Y., Gong, S. L., Shen, Z. X., Mei, F. M., Xi, X. X., Liu, L. C., Zhou, Z. J., Wang, D., Wang, Y. Q., and Cheng, Y.: Characterization of soil dust aerosol in China and its transport and distribution during 2001 ACE-Asia: 1. Network observations. *J. Geophys. Res.*, 108, 4261, doi:10.1029/2002JD002632, 2003.
- Zhang, X. Y., Wang, Y. Q., Zhang, X. C., Guo, W., and Gong, S. L.: Carbonaceous aerosol composition over various regions of China during 2006, *J. Geophys. Res.*, 113, D14111, doi:10.1029/2007JD009525, 2008a.
- Zhang, Y., Schauer, J. J., Zhang, Y., Zeng, L., Wei, Y., Liu, Y., and Shao, M.: Characteristics of particulate carbon emissions from real-world Chinese coal combustion, *Environ. Sci. Technol.*, 42, 5068–5073, doi:10.1021/es7022576, 2008b.
- Zhao, B., Wang, P., Ma, J. Z., Zhu, S., Pozzer, A., and Li, W.: A high-resolution emission inventory of primary pollutants for the Huabei region, China, *Atmos. Chem. Phys.*, 12, 481–501, doi:10.5194/acp-12-481-2012, 2012.
- Zhao, Q., He, K., Rahn, K., Ma, Y., Jia, Y., Yang, F., Duan, F., Lei, Y., Cheng, Y., and Wang, S.: Dust storms come to Central and Southwestern China, too: implications from a major dust event in Chongqing, *Atmos. Chem. Phys.*, 10, 2615–2630, doi:10.5194/acp-10-2615-2010, 2010.